Fabrication of Biocompatible Electro-conductive Silk Films with Natural Compounds for Tissue Engineering Applications

A thesis

submitted by:

Nikolaos Dimitrakakis

In partial fulfillment of the requirements for the degree of

Master of Science

In

Biomedical Engineering

TUFTS UNIVERSITY
February 2015

Adviser: David Kaplan

Copyright Notice

Abstract

In the present study electro conductive natural compounds are incorporated in silk based films, and the effects on film conductivity and dissolution are studied. Natural conducting compounds melanin and riboflavin were blended with silk to increase conductivity. Other compounds such as Fe(0) powder ferrofluid and NaCl solution also improved conductivity. Film properties and dissolution were studied for the different blends, and tuned using addition of glycerol and horseradish peroxidase cross-linking. Techniques such as electrospinning, doctor blade, spin coating, and paper-like film fabrication techniques were also explored to generate films with controlled dimensions and properties.

The findings suggest that the incorporation of riboflavin along with NaCl and glycerol in silk films, along with water vapor annealing results in semiconductor films. More specifically, the two compositions of the films that exhibited highest conductivity contain 2 % w/v silk, 20 % w/v glycerol, 2 % w/v polyethylene oxide (PEO), 30 % v/v phosphate buffered saline (PBS) and 5 % w/v silk, 20 % w/v glycerol, 10 % w/v NaCl with conductivities of $5.72*10^{-2}$ S/m and $5.96*10^{-2}$ S/m at 20 °C. When silk is doped with riboflavin, NaCl, and glycerol, semiconducting behavior similar to drinking water conductivity is observed.

Mass loss studies of the films included the immersion of the films for 7 days in 37° C in PBS. Film processing included samples that were heated for 2 hours in 60 °C immediately after casting, as well as those cured at room temperature. The results indicated that the heated samples provided the lowest mass loss of approximately 27 %.

In conclusion, the present study demonstrates the correlation between composition and processing of silk films with their conductivity. These semiconductive films have the potential to be applied in tissue engineering applications such as nerve conduits, where conductivity plays an instrumental role in tissue restoration.

Acknowledgments

The current thesis represents the work that has been conducted from October 2013 until April 2014 at Professor Kaplan's lab in the Department of Biomedical Engineering at Tufts University. During the whole period of my studies at Tufts I had the pleasure and luck to work and collaborate with brilliant people. First and foremost, I would like to thank Professor David Kaplan for his mentorship and for giving me the opportunity and honor to be part of his group and gain important experience and knowledge in the field of Biomedical Engineering. I also want to thank Dr James D White, for teaching me cell cultures techniques, for sharing many hours of discussion and ideas and for being there all the time advising, guiding me and answering my questions. Also, special thanks to Antonio Varone for his solidarity and support in many ways, and to my friend Nikos Fourligas who really believed in me; without his help I would not be able to complete my studies. The committee members, Professor Qiaobing Xu and Professor Tim Atherton for their kindness and willingness to be members of my thesis committee. Many thanks also to Professor Christian Staii for his help along with Dr. Elise Spedden with the Keithley meter and AFM. Special thanks also to Emma Schneider for her significant contribution in editing the present Thesis.

Last but not least I would like to thank all the members of Kaplan Neuro Tissue Group for their help in the lab and during the unforgettable meetings and everyone in Sci-Tech who have helped me in different ways during my studies.

Concluding, above all I thank and pray to God for being healthy and able to complete my studies and efforts at Tufts University.

A note from the author

Writing a Thesis is a challenging procedure, not only because of the load of work and the time that it takes to be accomplished, but also because it should be written in way that is attractive and friendly to the reader. The ultimate goal is to manage demonstrate the results and transfer the scientific approach and mentality of the study in an easy way. Considering this, the author followed the "visual approach" of the concept which emphasizes in the inclusion of many figures. The author believes that a text rich in figures acquires another dynamic and interaction with the reader. Moreover, images supplement and often explain the text, giving another dimension in the perception of phenomena, experiments and results. Otherwise, "A picture is worth a thousand words".

Concluding we believe that this work explored a large amount of different mixtures and compounds and also alternative processes, (especially given the time frame that this workload has been conducted). Any constructive criticism is always welcome.

Nikolaos Dimitrakakis

"I know one thing: that I know nothing"

SOCRATES

Table of Contents

List of Figures

List of Tables

List of Abbreviations

ECM	Extracellular Matrix
PGS	Polyglycerol Sebacate
RGD	Arginyl-glycyl-aspartic acid
hMSC	human Mesenchymal Stem Cells
PEO	Polyethylene Oxide
PBS	Phosphate Buffered Saline
BMP-2	Bone Morphogenetic Protein 2
PAc	Polyacetylene
PPy	Polypyrrole
PANI	Polyaniline
PTh	Polythiophene
PPh	Polyparaphenylene
PPhV	Polyphenylenvinylene
SN	Polysulfur Nitride
Eg	Energy Gap
Tyr	Tyrosine
L-DOPA	L-3,4-dihydroxyphenylalanine
DHI	5,6-dihydroxyindole
RDAs	Recommended Dietary Allowances
PTFE	Polytetrafluoroethylene
NGF	Nerve Growth Factor
PDMS	Polydimethylsiloxane
HRP	Horseradish Peroxidase

MW	Molecular Weight
MeOH	Methanol
UV	Ultraviolet
SEM	Scanning Electron Microscopy
S/cm	Siemens/centimeter unit of conductivity (S = 1/R , where R=Resistance)
w/v	weight over volume
v/v	volume over volume
DI	De-Ionized
DPBS	Dulbecco's Phosphate-Buffered Saline
HEPES	(4-(2-hydroxyethyl)-1-piperazineethanesulfonic acid)
DMSO	Dimethyl sulfoxide
SN	Polysulfur Nitride
rpm	rads per minute

1. Introduction

1.1 Silk as a biomaterial

Silk fibroin has been used for centuries in applications of textile to medical accessories due to its high tensile strength and elasticity [2]. It creates an excellent support matrix for therapeutic delivery agents and scaffold design and gives promising results to obtain the similar functional properties as the extracellular matrix (ECM) [3]. The complexity of the ECM interactions makes it hard to mimic for multiple biological activities [1]. However, unlike the other polymers specifically design to exhibit tunable mechanical properties resembling the native cell matrix, silk fibroin is amongst the few that is biocompatible, biodegradable and easy to modify for incorporation of biologically active properties [3]. Unlike polyglycerol sebacate (PGS), which is a promising biomaterial to be used as a platform for nerve regeneration [4] but has a disadvantage of quick clearance, silk fibroin can be used as a long-term scaffold due to its controllable, long-term degradation profile [6]. With this being said, silk also has an advantage of showing no cytotoxicity upon degradation, which is the opposite case for many synthetic polymers that are commonly used as biomaterial scaffolds [1]. Thanks to the advances in silk fibroin extraction from cocoons of *Bombyx mori* silkworm, water based extraction techniques make silk fibroin a suitable candidate for non-cytotoxic and durable biomaterial as well as easy to obtain in large quantities [2].

For ECM interactions, silk shows an inert profile like synthetic polymers although it is a natural, biocompatible protein. Silk does not contain any biologically active recognition sequences therefore shows no immunogenic profile [5]. Yet, the ability to modify silk for any desirable activity is shown to be easy via known functionalization techniques.

Arg-Gly-Asp (RGD) functionalization is used for scaffold cell interactions to facilitate cell attachment and easy cell proliferation [7,8]. Blending with other chemical agents and biocompatible polymers either covalently or physically allows the formation of a bio-platform with desired function such as elastin-silk polymer blends [9] for tunable mechanical properties, collagen-silk blends [10] for both cell attachment and ECM interactions.

Unique β-sheet formation of silk fibroin creates many different silk materials in different forms. Hydrogen bonding (H-bonding) driven β-sheet formation in silk stems from its hydrophobic nature. Hydrophobic chains pack closer together allowing easier H-bonding formation between the chains, creating crystalline form. Orderly structured β-sheet crystals give rise to the durability of the silk materials [11]. The most popular crystallization treatments are water vapor annealing, and methanol treatment. Sonication also has been used in silk solutions for controlling the silk fibroin gelation [82]. To date, silk films, fibers, silk hydrogels, scaffolds, microspheres have been created and proven to be useful for different applications such as drug delivery, and coating materials [2].

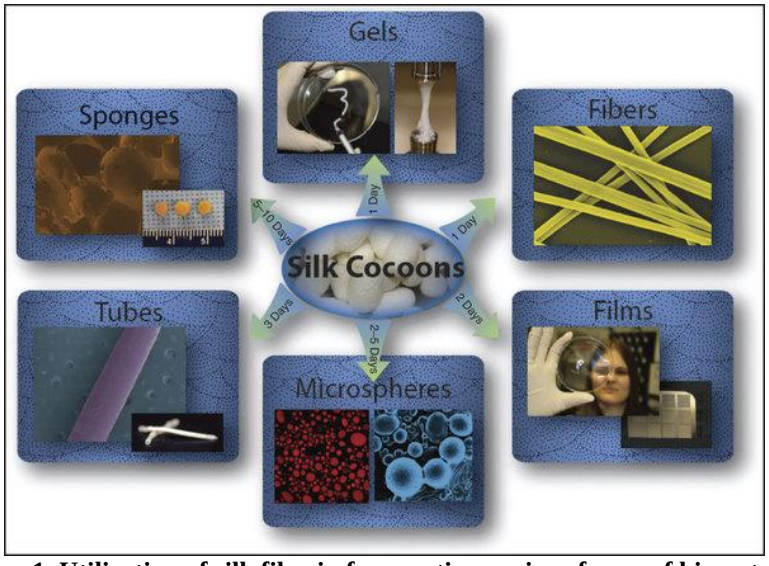

Figure 1. Utilization of silk fibroin for creating various forms of biomaterials [1].

Silk films are excellent platforms to screen cell differentiation *in vitro* due to the ease of 2D cell culture and apply to different conditions of interest such as different growth factors and chemicals, thanks to the excellent oxygen and water permeability of the silk films. Previously, human mesenchymal stem cell (hMSC) adhesion and proliferation has been shown on silk films. When electrospinning, Polyethylene oxide (PEO) is blended to increase roughness and provide cell attachment [14]. Especially for bone formation, RGD and bone morphogenetic protein 2 (BMP-2) [12,13] incorporation in to the silk, showed increased cell attachment and higher differentiation.

Fabricating electroconductive biomaterials with easy-to-tailor properties for various tissue engineering applications is one of the major and important goals for tissue engineers. In particular, in conditions such as peripheral nerve injury, the neuro tissue engineering approach offers a new perspective for the nerve restoration and regeneration, creating a new area of research [16].

The functionalization of silk films with electroconductive properties will advance further this excellent material and will offer new potential in applications such drug delivery devices, biosensors and neural implants [17].

1.2 History and evolution of conducting polymers

Polymers are chemical compounds that consist of macromolecules with large number of identical chemical units (monomers) linked by covalent bonds. The polymers exhibit a variety of properties, which makes them particularly suitable for technological applications. Some of the interesting properties are ease of molding, electrical and thermal conductivity, changes in properties with temperature, and moisture absorption. Generally, the value of a certain property depends not only on the specific polymer, but also on the method used for synthesis [24].

Until 1973, all known polymers were good electrical insulators and used extensively for electrical insulation. However, the same year Labes M.M, Love P. and Nichols L.F. discovered that the inorganic polymer polysulfur nitride $(SN)_x$ exhibited metallic conductivity. The value of the specific conductivity at room temperature was in the order of 103 S/cm, while in 1977 discovered that in 0.3 K this polymer becomes superconducting. The metallic nature of this polymer is an intrinsic property and is connected to the existence of an uncoupled electron per SN unit, which can be moved along the chain [15].

The inorganic $(SN)_x$ was then replaced by organic conductive polymers whose discovery began in 1974 coincidentally after a mistake. The Hideki Shirakawa, Institute of Technology, Tokyo, was trying to synthesize polyacetylene from the usual fuel acetylene. This polymer, a tan powder was synthesized for the first time in 1955, but no one expected it to have an interesting application. Instead of a tan powder, Shirakawa saw surprisingly a glossy silver film that resembled aluminum foil which maintained elasticity of transparent polyacetylene film [25].

Ultimately, this was due to an error during the synthesis process, where a thousand times more catalyst was added in the instructions.

The new form of polyacetylene was investigated by Shirakawa, MacDiarmid and Heeger in 1976 and found that by adding iodine in the material (doping), the silver leaf films, took a gold color and the conductivity increased over 1,012 times. Polyacetylene, which is the simplest conductive polymer, is considered the standard of these materials because it has been extensively studied and displays higher electrical conductivity than any other polymer [15].

The importance of the discovery was recognized with the award of the Nobel Prize "For the discovery and development of conductive polymers" in 2000 to the aforementioned researchers. The realization that conductive polymers can be as light material conductors of electricity, which can replace metals in many applications, gave a boost to the synthesis of other polymers with conductive features using various fabrication methods [19]. To emphasize the conductive properties of these polymers was introduced the term 'synthetic metals' to describe this emerging family of materials. The investigation of polymer conductive materials, which possess good mechanical properties, has continued with unflagging interest for various applications in the field of tissue engineering and for the theoretical understanding of the structure and conductivity.

Typical characteristics of the conductive polymers are the alternating single and double bonds along the main chain, leading to a wide π-electron conjugation [20]. Therefore, polymers with the above property are known as conjugated polymers. The main representatives of the broad family of conjugates are polyacetylene (PAc), polypyrrole (PPy), polyaniline (PANI), polythiophene (PTh), polyparaphenylene (PPh), polyphenylenvinylene (PPhV). However, these polymers do not exhibit conductivity in the neutral (uncharged) state and transition to the conductive phase should be enriched with conductivity carriers/dopants [21]. The possibility of enrichment or doping of the polymer conjugates plays a central role in their discrimination from all other polymers.

The low production cost, ease of production and molding, in combination with good mechanical properties, enable the conductive polymers used in numerous technological applications, replacing conventional inorganic semiconductors and metals [21, 26].

The conductivity results from the formation of conductivity carriers through oxidation (enrichment type p) or reduction (enhancement type n) of the conjugate chain. The ability of adding impurities for the controlled enrichment of the conductive polymers is due to the fact that the forces among polymer macromolecules are weak, allowing the diffusion of molecules and impurities in the mass of the polymer [22].

It is known from the classical theory of zones that the energy levels of electrons in a crystal form zones [19]. The zones are separated energy gaps. These energy gaps separate into two zones, one which is completely filled and called the valence band the other of higher energy which may be empty or partially filled and called the conductivity zone.

Insulators are characterized by a wide energy gap and therefore the electrons, the conductivity carriers, cannot pass. In semiconductors, the energy gap is narrow so the electrons are able to move in the conductivity zone through energy excitation. Thus in semiconductors, as well as metals, the level of conductivity is partially filled. The application of an electric field results in the conduction of current.

The formation of the energy gap is explained by taking into account either the interactions of electrons-photons or electron-electron interactions between π-electrons [23].

In these materials the energy gap (Eg) is a few electronvolt (eV) and overlaps with relatively small supply of potential. Semiconductors at low temperatures are poor conductors of electricity, while at high temperatures; they are good conductors [27].

In semiconductors in absolute zero temperature the valence band is complete. Consequently, in the conductivity band zone there are no electrons. However, at ambient temperatures, the thermal energy provided is sufficient to cause the electrons jump from the valence band to the conduction band. When an electron jumps from the valence band to conductivity band, an electronic hole is created. The electrons, that switched to the conductivity zone and the empty energy holes they left in the valence band are the carriers of conductivity of the semiconductors [27,28].

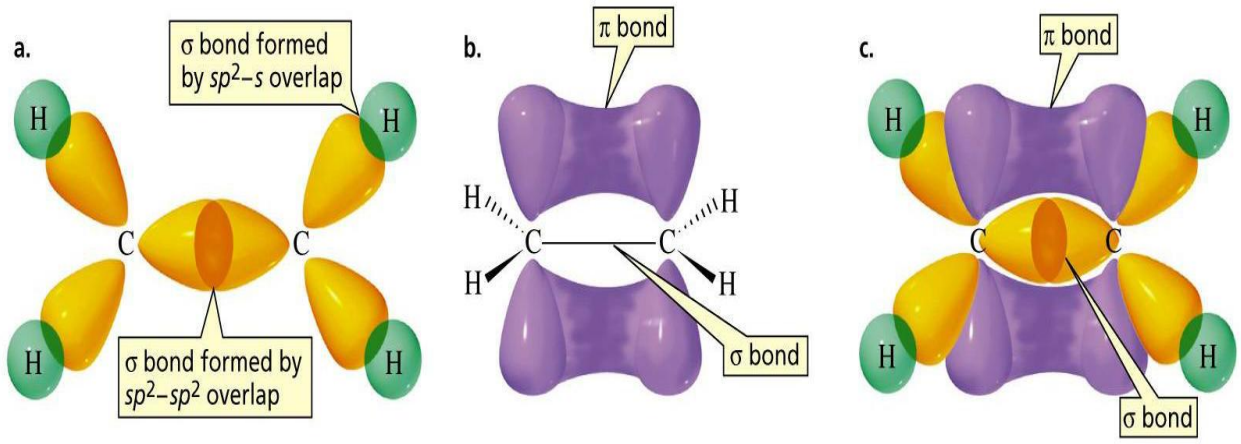

Figure 2. Molecular mechanism of biopolymer conductivity. Conductive properties of (bio)polymers are due to π bonds that occur across the polymers chain (π-conjugated molecules and polymers) [29].

As it shown in Figure 2 the valence carbon electrons interact to form one of the sp, sp^2 or sp^3 orbitals. The double bonds between 2 carbon atoms occur from the overlapping of sp^2 orbital. In a pure crystal, the number of the intrinsically produced free electrons is obviously equal to the number of holes. This type of semiconductor is called an intrinsic semiconductor [27,28].

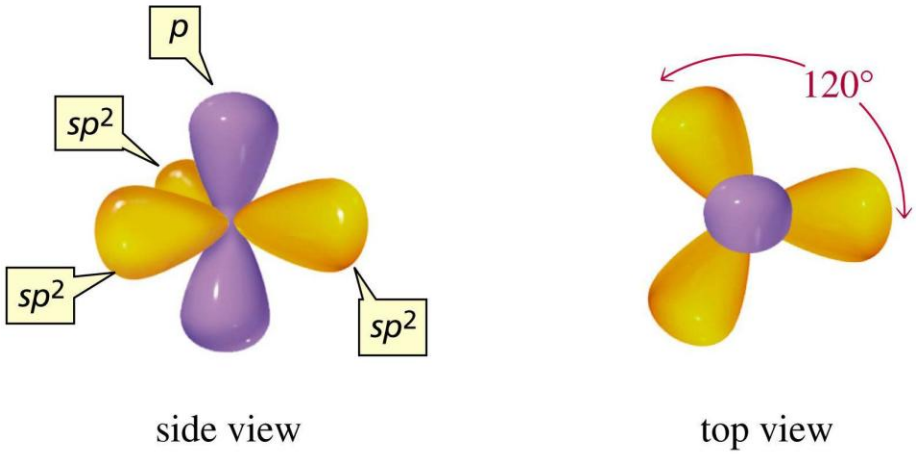

Figure 3. Side and top view of the orbital's and bond angle [29].

For this purpose, in the crystalline lattice of the material, foreign compounds are introduced. In this way electroconductivity is improved and can be adjusted proportionately with the amount of the foreign compound added. These types of semiconductors are called extrinsic semiconductors and are two kinds [26,28]:

1. The n-type if the carriers in the semiconductors are electrons
2. The p-type if the carriers are the holes.

1.3 Semiconductors: n-type

Semiconductors of this type are the main carriers of free electrons, generated when atoms with greater than 1 valence electron are introduced into the intrinsic semiconductor crystal lattice.

These free electrons, which do not participate in covalent bond with neighboring atoms, can easily jump into the conduction band, where they behave as a free charge carriers. The electron that is now excited into the conduction band leaves behind an ionized atom that is called donor because it donates the electron to the conductivity band [29,31].

The bands of the donor electrons are very close to the conductivity band of the semiconductor, a fact that justifies the jump of these electrons to the conductivity band. For this reason, the Fermi level of the extrinsic semiconductor moves towards the conductivity band, as shown by the energy diagram in Figure 4 [26,27,29].

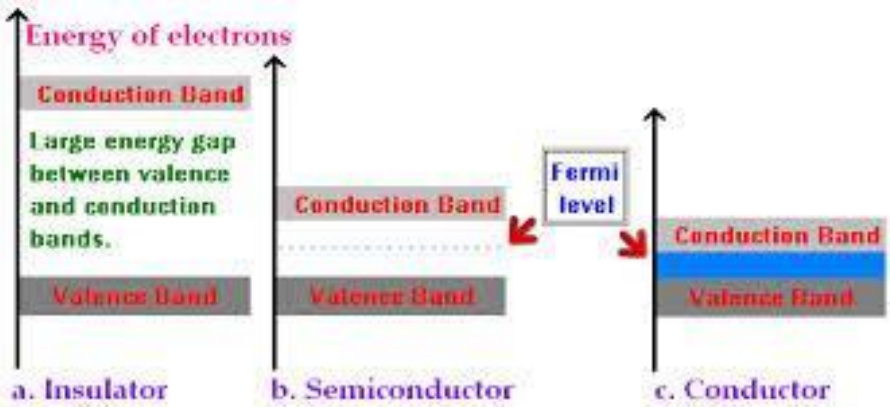

Figure 4. Electron bands width and Fermi level for a. insulator b. semiconductor c. conductor. Smaller energy gaps means lower potentials for conductivity [27].

An important observation is that there is not a corresponding hole for every electron in the valence band, as in the case of endogenous semiconductors. Therefore the concentration of n free electrons is greater than the concentration of p holes. This usually happens due to the impurity concentration of foreign atoms than the concentration of the n intrinsic carriers and this determines the specific conductivity of the semiconductor [27,28,29].

1.4 Semiconductors: p-type

P-type semiconductors are generated when atoms with at least 1 valence electron are introduced into the intrinsic semiconductor crystal lattice. In correspondence with the semiconductor type n, covalent bonds are generated between these atoms and the adjacent atoms.

However, due to non-completion of a covalent bond, is generated a hole instead of electron. In this case the amount of p holes is greater than the amount of n electrons and the holes are the charged carriers. The atoms of the elements that are introduced are called receptors [27, 30].

The levels of the electrons of the receptor are located in the valence band of the semiconductor. This fact justifies the jump of electrons from the valence band of the semiconductor to the bands of the electrons of the receptor. The Fermi level of the exogenous p-type semiconductor is not located in the middle of the energy gap but closer to the band zone [28,30].

Concluding n-doping cannot occur in ambient conditions. The oxygen-rich atmosphere creates an oxidizing environment. A polymer that is n-doped and rich in electrons will de-dope (reoxidize to the neutral state) the polymer. In order to achieve n-doping, the environment contain an inert gas (e.g. argon). In research what is usually applied is electrochemical n-doping, because it is easier to create an environment with low oxygen concentration (sealed flask or under vacuum). Silk doping with the doping agents in this study falls under the category of p type doping.

In the study of electrical conduction in biopolymers it is important to have an accurate and reliable method to determine the conductivity or its reciprocal, resistivity. Although instruments allow the resistance of the sample to be determined experimentally, the materials property of interest is the resistivity, p, which is the resistance between the opposite faces of a unit cube of the material and has units of Ω m [18,19,20]. The conductivity, σ, is defined similarly and has units of Ω^{-1} $m^{-1.}$ The conductivity of materials varies over a wide range.

Insulators have conductivities typically less than 10^{-12} S/m, semiconductors are in the range 10^{-12} S/m to around 10 S/m and the conductivity of metal is greater than about 10 S/m .

It can be seen that polymers are now available in a full range of conductivities found in other materials as well [19,20].

1.5 Doping compounds

Material	Control Properties	Electrical Conductivity	FDA Approval	Biocompatibility	Biodegradability	Mechanism Conductivity	Efficiency
Melanin [37,38,39]	Cons: Lack of solubility in many organic solvents Pros: Solution processing of melanin into device-quality films is made possible by using aqueous ammonia preparations	Relatively high		Melanin films induced an inflammation response that was comparable to silicone implants in vivo. Furthermore, melanin implants weresignificantly resorbed after 8 weeks.	Melanin films degrade in vivo	Hydration mediated proton transport biomaterials based electronics	Melanin films prepared by spin coating promote neurite extension from PC12 cells that exceeds the length of neurites extended from PC12 cells cultured on collagen films
Poly-L-tyrosine [40,41,42]	Can be controlled except temperatures well below the glass-transition temperature and for small currents	Demonstrates conductivity	Poly(DTE carbonate)(desaminotyrosyl-tyrosine ethyl ester) is expected to be the first tyrosine-derived polymer to become commercially available for clinical use.	No sign of cytotoxicity	Fast biocompatibility	The phenol group in tyrosine undergoes oxidation, losing two protons and two electrons in a two-step process	
PEDOT poly(3,4-ethylenedioxythiophene) doped [43,44,45]	Excellent chemical stability in aqueous solution at room temperature even at higher temperature, transparent	Exhibits high conductivity and stability in the oxidized state	is being sought (when it is doped with poly(styrene sulfonate)(PEDOT:PSS))	Highly biocompatible, has beedn used also within hydrogels	Not degradable	p-doping where removal of one electron creates a positively charged "hole" that acts as a charge carrier in the polymer. This can be accomplished by the addition of negatively charged counter ions	PEDOT can promote neurite outgrowth by providing physical and/or electrical growth cues
Polyaniline [45,46]	Diversity of structural forms, high environmental stability and ease of charge transport	Relatively high, has been shown that it is a suitable electroactive conductive substrate for cardiac cell		It is biocompatible showing cell and tissue compatibility in vivo and in vitro syStems	Not degradable		PAni exhibits th fact that cardiac cells grow equally growth well on TCP and Pani may not be generalized to all cell types

Table 1. Presentation of the properties of candidate compounds for conjugates[37-46].

After searching for candidate compounds that could be utilized to provide conductivity to our films, the following biologically active molecules were chosen: iron, melanin, riboflavin and NaCl. The criteria of this selection are the naturally derived, biocompatible, degradable, and have demonstrated electrical conductivity.

Moreover, to the best of our knowledge it is the first time that these molecules have been investigated in conjugation with silk as well as in blends with iron and NaCl for electro conductive bio-applications.

1.5.1 Riboflavin (Vitamin B2)

Riboflavin (6,7-dimethyl-9-(D-1-ribityl)-isoalloxazine) is commonly known as Vitamin B_2 it is a natural pigment, polar and therefore soluble in water with the chemical formula $C_{17}H_{20}N_4O_6$. Its polarity derives mainly from four hydrogen bonds between hydrogen and oxygen and also the two polar bonds between oxygen and carbon, and the polar bond between hydrogen and nitrogen.

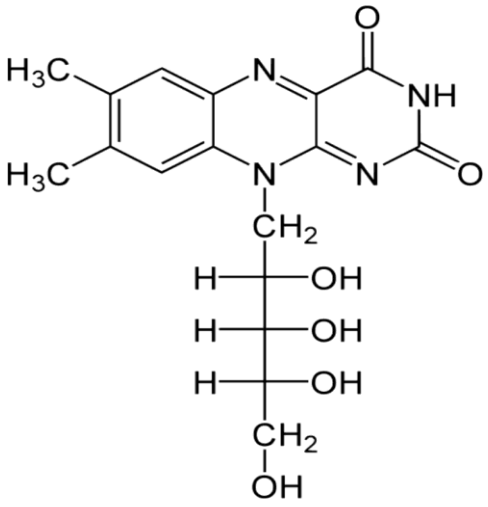

Figure 5. The chemical structure of riboflavin [47].

Riboflavin has been investigated for the its electrochemical properties [47,48]. Riboflavin is capable of accepting either one electron in a two-step process or two electrons at once.

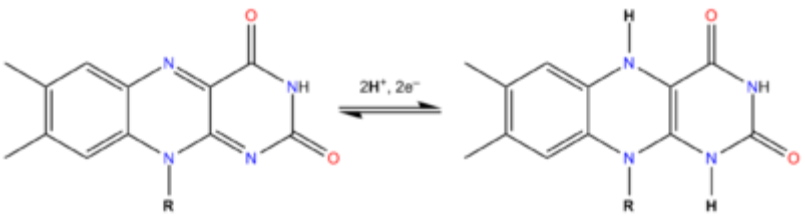

Figure 6. Oxidative-reduction reaction of riboflavin. On the left oxidative form of riboflavin and reduced form on the right [48].

1.5.2 Melanin

Conjugation in polymers created a whole new class of conducting materials. Electrical conductivity of this new class of polymers stems from the electron delocalization in the p orbital and the ease of electron transfer that differs them from the oxidation/reduction behavior of the conductive inorganic materials. The ability of organic materials to conduct electricity enables new materials to be synthesized for bio-related applications [49].

Melanin is one of those conductive biomaterials with a conjugated backbone. Its amorphous structures enable it to solubilize in water. Melanin is commonly found in the vertebrates, plants and animals as a pigment that gives the skin its color. Based on polymer classification, melanin falls under the carbonaceous polymers since it has an organic backbone that includes humic and fulvic acids as well as polycyclic aromatic hydrocarbons [50].

There are two main types of melanin based on color: pheomelanins and eumelanins. Eumelanins are the most common type that is black due to the pigment they carry and they have higher molecular weight. Humans synthesize melanin from a special cell type called melanocytes. Melanines are found in the cytoplasm of melanocytes in special parts called melanosomes.

The predominant structure in melanin is an indole subunit with 5,6-dihydroxyindole (DHI) [49,50,51].

A more detailed synthesis of melanin starts with the oxidation of tyrosine (Tyr) by tyrosinase to L-3,4-dihydroxyphenylalanine (L-DOPA). Then L-DOPA is oxidized to its quinine form, then via Michael addition resulted in intramolecular cyclization into dopachrome. Tautomerization of dopachrome gives leucodopachrome and oxidized into 5,6-dihydroxyindole (DHI). In the laboratory, the synthesis starts from L-DOPA, eliminating the oxidation of tyrosine into side compounds [50].

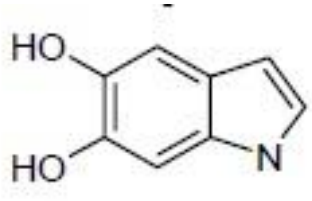

Figure 7. 5,6-dihydroxyindole (DHI) [57].

Melanin consists of 5,6-dihydroxyindole (DHI) via covalent linkages thus results in a conjugated backbone. It is a conjugated polymer made up of a conductive monomer. A threshold switch that is mostly seen in semiconducting inorganic materials (and lately in synthetic polymers) was seen with melanin back in 1974 [49]. Melanin showed conductivity similar to inorganic materials (only 2 orders of magnitude lower) but also it showed a reversible reaction. In other words, the bioorganic material did not break down or degrade. In 1982, Strzelecka proposed a band model for synthetic melanin and compared the conductivity of bioorganic melanin extracted from various living organisms and synthetic melanin [50,52].

She found that synthetic melanin has a higher conductivity (3 orders of magnitude), possibly due to the foreign material present in the extracted bioorganic melanin such as other insulator proteins [51].

Osak et al. revealed that there are traps in the melanin polymer that results in electrical conductivity via conjugation determined with current-voltage (I-V) measurements [53]. Another study with pheomelanins, which is showing the same conductivity band as the bioorganic melanin, was conducted by Jastrzebska et al. [54]. She found that the previously lower values for the pheomelanins were due to the disorder of the structure caused by benzothiazine. Pheomelanin also shows photoconductivity [55].

Rosei et al. studied synthetic dopa-melanin and found the structural characteristics [56]. The conjugated π network of melanin has been shown to have conductive properties.

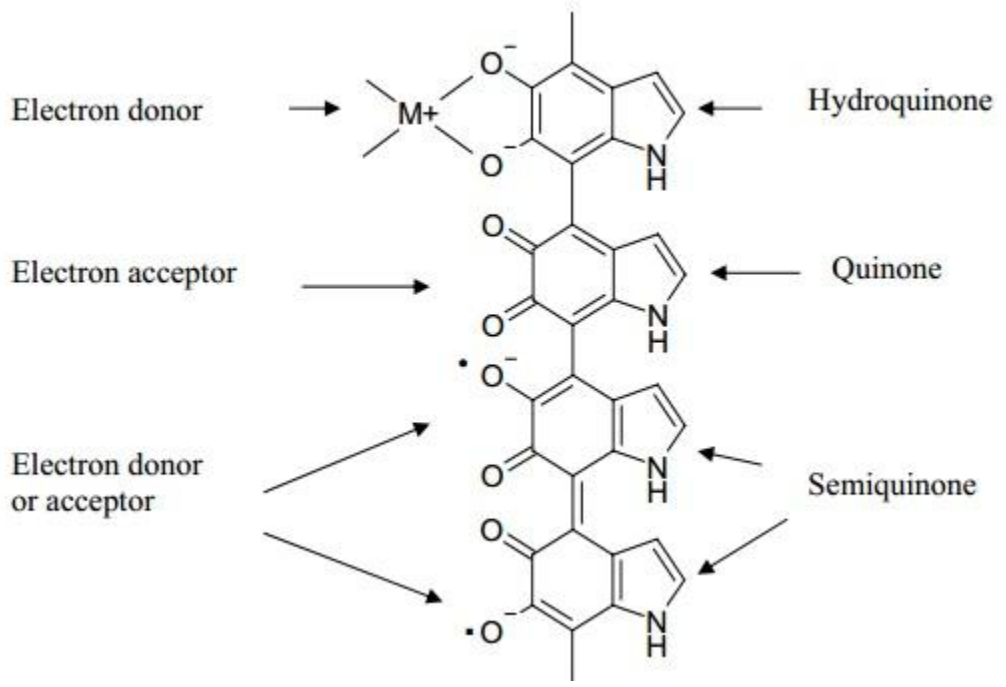

Figure 8. Melanin as electron donor or acceptor [59].

Another important study regarding the water interactions of melanin was done by Jastrazebska et al. [58]. They found out that conductivity of melanin increases with humidity by 8 orders of magnitude. The presence of water molecules within the indole quinone monomer layers that are held tightly via H-bonding increases electron transfer, therefore increasing the conductivity.

The conductive properties of melanin and its potential use as a substrate in tissue engineering has been studied by Bettinger et al. [38]. However, there are limited studies for the utilization of melanin as a dope in biomaterials. Lack of studies increased the interest to investigate melanin as a dopant in silk films.

The preliminary idea to conjugate silk with melanin was based also in the hypothesis that the serine-OH found in the structure of silk will attack the COOH found in melanin molecule to produce esters (Fischer esterification, Figure 9).

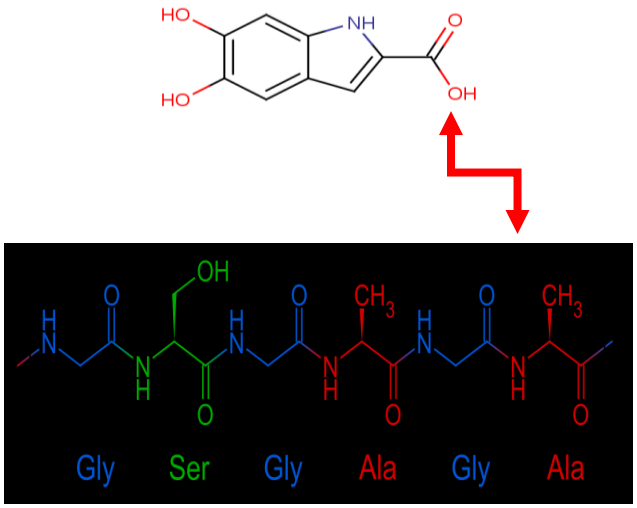

Figure 9. The hypothesis that the serine groups found in silk will replace the COOH in melanins producing ester (Fischer esterification).

1.5.3 Glycerol

Glycerol is an empirical chemical name of the organic compound propane 1,2,3-triol, which is a trivalent alcohol. The glycerol molecule contains three hydroxyl groups, which result in high solubility in water and hydrophilic nature. Generally, the glycerol is a starting material for plethora of chemical process and also in biomedical applications where it is used as a plasticizer, wetting agent and solvent.

In biomedical applications glycerol has good compatibility and it is non-volatile. In these processes it reacts with two ways, the first one is its reduction or oxidation to 3 carbon atoms and the second is its reaction with other compounds [60].

The use of glycerol in biomedical applications and in combination with silk has been studied by Tsukada et al. [61], Lu et al. [62] and Yun et al. [63]. In these applications glycerol offers multiple desirable properties. One of the most important properties is that it works as a plasticizer and reverses the brittle behavior of the polymer, making materials more flexible [63]. Tsukuda et al. have also observed that glycerol is acting as wetting agent which prohibits the1 further wetting in aqueous environment and thus suppresses the degradability of the materials. In the same work the affect of glycerol increased the conductivity [61]. Lu et al. [62] also demonstrated the blending of silk and glycerol without the use of organic solvents and they found that glycerol stabilizes the silk films and also adds to them beneficial properties such softness and morphologies that can be easily modified [62].

1.5.4 Fe(0) powder

Another natural compound that was incorporated with silk is solid Fe(0) powder. Iron is an essential element for the human body. It is a necessary component of hemoglobin in red blood cells that is a protein responsible for carrying oxygen from lung to the tissues. Lack of iron can cause anemia, and also limits the carrying capacity of blood. However, exceeding the daily-suggested amount of iron can be very toxic for the human body because it boosts the generation of free radicals [64]. The Recommended Dietary Allowances (RDAs) for iron is between 8-18 mg [65]. Iron has been widely used in many applications where conductivity is required.

1.5.5 Ferrofluid

Ferrofluid is a colloidal liquid that has magnetic and electric properties. Ferrofluids are made of nanoparticles of different materials such as magnetite, hematite or other compounds that contain iron. The nanoparticles are suspended in an organic solvent or water. Aggregation of this nanoparticles is avoided by using a surfactant that coats each nanoparticle [67].

1.5.6 NaCl

Sodium chloride is formed due to the ionic bonds between Na^+ and Cl^-. Ionic bonds are a strong bond and therefore in ambient temperatures the ionic compounds are solids and have crystal structure. However, although these compounds consist of ions they do not exhibit electrical conductivity. Nevertheless, when NaCl is dissolved in distilled water it turns to a conductive solution.

This phenomena occurs because water molecules are inserted in between the ions of the crystal lattice of NaCl. Thus the crystal structure gets disrupted and the ions of Na^+ and Cl^- move freely in the solution. If voltage is applied with the electrodes the positive ions of sodium are attracted from the negative charged electrode and the negative ions of chloride are attracted by the positive charged electrode. These attraction forces cause a flow of ions to the electrodes which is the electrical current. Dissolving NaCl could potentially provide free ions that are entrapped with the film mass and act as charge carriers.

1.5.7. Polyethylene oxide (PEO)

Polyethylene oxide (PEO) is used in casting the silk fibroin films. Blending with PEO is chosen first to increase solubility of the silk and increase the homogeneity of the film throughout the spin coating process. Secondly, PEO is biocompatible and it eliminates the use of organic solvents. Thirdly, it can be extracted in the methanol or water annealing treatment where beta sheet formation is induced and insoluble crystal silk films form without the incorporation of water soluble PEO. Another advantage of blending with PEO are the inert characteristics of PEO does not interfere with the conductivity experiments [14].

1.6 Applications of silk films in neuro tissue engineering

The rehabilitation of injuries of the peripheral nervous system is a major challenge. Each year hundreds of thousands of people suffer from paralyzed limbs, result of peripheral nerve injury. Recently, the implantation of artificial nerve grafts has become the method of choice for the repair of damaged peripheral nerves.

However, this often causes pain in the implantation area, and it can be difficult to find a nerve segment that has the same diameter as the damaged nerve. Nerves can be obtained from another human, but can be rejected by the immune system of the recipient [33]. An alternative approach, which has appeared about the last ten years, is the use of artificial nerve grafts made of silicone or synthetic polymers such as polyethylene. These generate scaffolds that bridge the gap in the damaged nerve and function within conduits, which can be grown nerve fibers. The artificial and synthetic nerve grafts such as Polytetrafluoroethylene (PTFE) carry a degree of functional recovery, but they can become toxic over time.

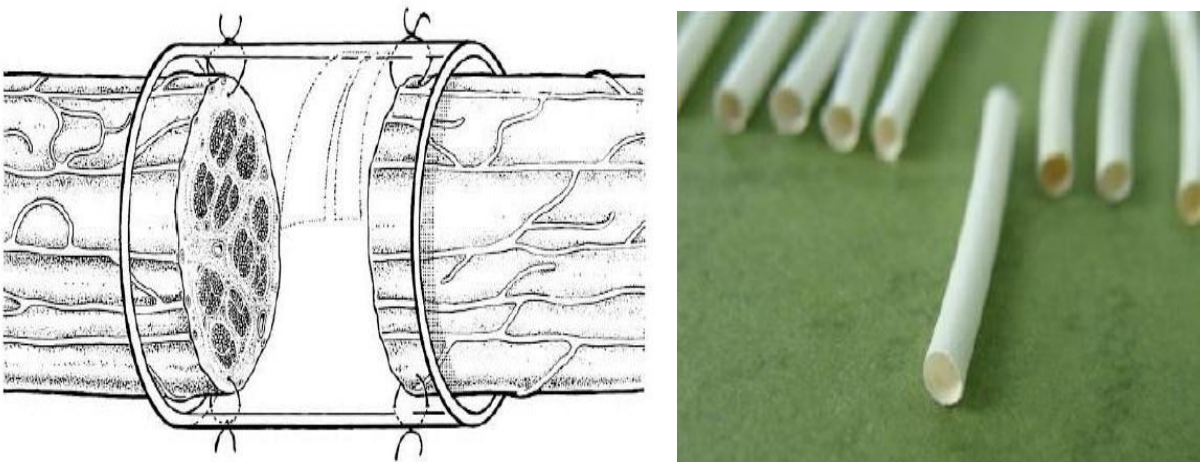

Figure 10. A. Nerve guidance conduit wrapping the nerve gap [35]. B. Nerve guidance conduits fabricated of silk fibroin via electrospinning [36].

These problems can potentially be overcome with the use of neural transplants which are made of natural components are biodegradable and biocompatible materials [32].

To overcome this limitation we aim to use silk fibroin as a biomaterial and create film-nerve conduits made of silk and other natural compounds such as riboflavin and melanin. Silk fibroin is a unique biomaterial that can be processed into numerous different physical states that can be used for tissue engineering applications.

As a biomaterial it is considered biocompatible (does not cause an inflammatory reaction) and biodegradable (degrades naturally *in vivo*) and also provides the ability to culture Schwann cells, a type of cells that is paramount in the development and regeneration of nerves [17,32,34,89]. Electrical stimulus increases the directional growth and the regeneration of neurons *in vitro*. Additionally, the degradability of the films will allows us to deliver drugs and growth factors such as nerve growth factor (NGF) that will contribute to the growth and regeneration of the neurons and are contained within the mass of the film [17,33,34].

2. Research objectives

The aim of this project is to develop silk fibroin films doped with natural compounds that can exhibit conductive behavior, are biocompatible, do not dissolve in aqueous solution and demonstrate flexibility. To achieve this goal, biologically conductive molecules were incorporated to silk fibroin in order to confer conductivity via conjugation or oxidation-reduction. Various processing and fabrication techniques were applied. The ultimate goals of this research is the applications of these doped silk films as nerve guidance conduits which can conduct electrical current and assist in the regeneration of damaged peripheral nerves.

3. Materials and Methods

3.1 Silk fibroin solution preparation

Silk fibroin solution was prepared from the *Bombyx mori* cocoons. The cocoons were boiled for 40 minutes in an aqueous solution of Na_2CO_3 to remove the protein sericin in combination with several thorough rinsing with Milli-Q water washes.

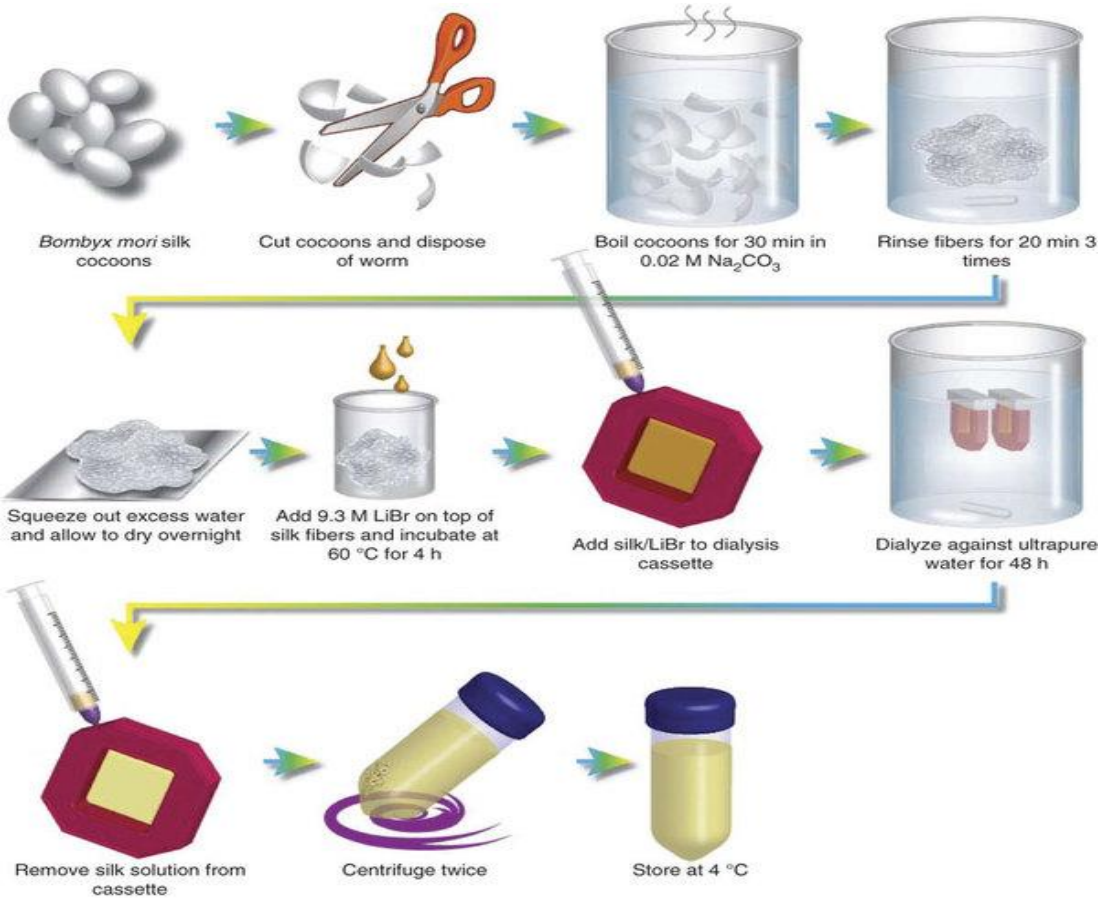

Figure 11. Process diagram of silk fibroin fabrication from Bombyx mori silk cocoons [2].

The cotton-look silk mass is dissolved in 9.3 M LiBr solution and placed in 60 °C for 4 hours. The resulting silk solution was dialysed against in Milli-Q water using dialysis cassettes for 48 hours to remove the remaining LiBr [2].

After dialysis the new diluted solution was centrifuged at 8,700 rpm for 20 min at 4 °C for further purification and additional removal of particulate. Finally, 0.5 ml of silk solution was sampled and dehydrated in 60 °C and then weighed to determine the concentration. With the aforementioned procedure, a solution of 7-8 % w/v was obtained. Further concentration of silk was done by using dialysis cassettes in order to achieve 10 % w/v concentration. Evaporation of water was achieved by placing them under the chemical hood to for 2-3 hours [2].

3.2 Preparation of silk films

3.2.1 Preparation of polydimethylsiloxane (PDMS) casting substrates

PDMS substrates were prepared for the casting of silk films. The PDMS molds were created by mixing 180 grams Sylgard® silicone elastomer base (Dow Corning Corporation) with 20 grams of the respective elastomer curing agent upon a 625 cm^2 square polystyrene pattern mold (Figure 13) or Petri dishes resulting 3mm thick flat PDMS substrates. The cast mixture of elastomer and epoxy of PDMS was placed under vacuum for 2 hours for releasing the bubbles with the mass of the liquid and then placed under then at 60 °C for 24 hours to be cured. Following curing, PDMS molds were removed from the polystyrene mold and cut into round geometries with the use of a biopsy punch 25.5 mm diameter. The PDMS molds were used multiple times for multiple castings of silk films. After every use they were washed with detergent, dried, wiped and rinsed with 70 % ethanol to remove any residues from the previous films that were cast [72].

3.2.2 Preparation of silk film solution with natural conducting dopants

To be able to perform conductivity measurements by altering the length of the two points of measurements the fabrication of 1 ml of solution which was cast in 25.5 mm molds giving various thicknesses of films ranging from 0.1-0.7 mm. More specifically, Wheaton Cryotubes tubes of 2 ml volumes were used for solution mixing to provide better mixing with the baffles in their interior. Stirring was applied with the aid of vortex and better mixing was achieved. In some cases as it is presented later, sonication was also applied to increase solubility, dispersion and mixing of the ingredients. In the case of sonication were used falcon tubes of 15 ml and the volume that was used was 5 ml. The silk fibroin solutions along with riboflavin were load for sonication in 15 ml transparent falcon tubes. The films were cast on the PDMS molds (Figure 13). The molds were kept in a fume hood generally for 48 hrs with stable airflow 0.2 m/s at room temperature to ensure consistent evaporation and drying of films. All the films prepared after peeling of PDMS substrates were taken for conductivity measurement and then kept in petri dishes sealed with parafilm and stored at room temperature. The solution mixing technique that is described above was used in all the films that were cast with all the different dopants.

The protocol followed generally for mixing solutions it is presented below (Figure 12).

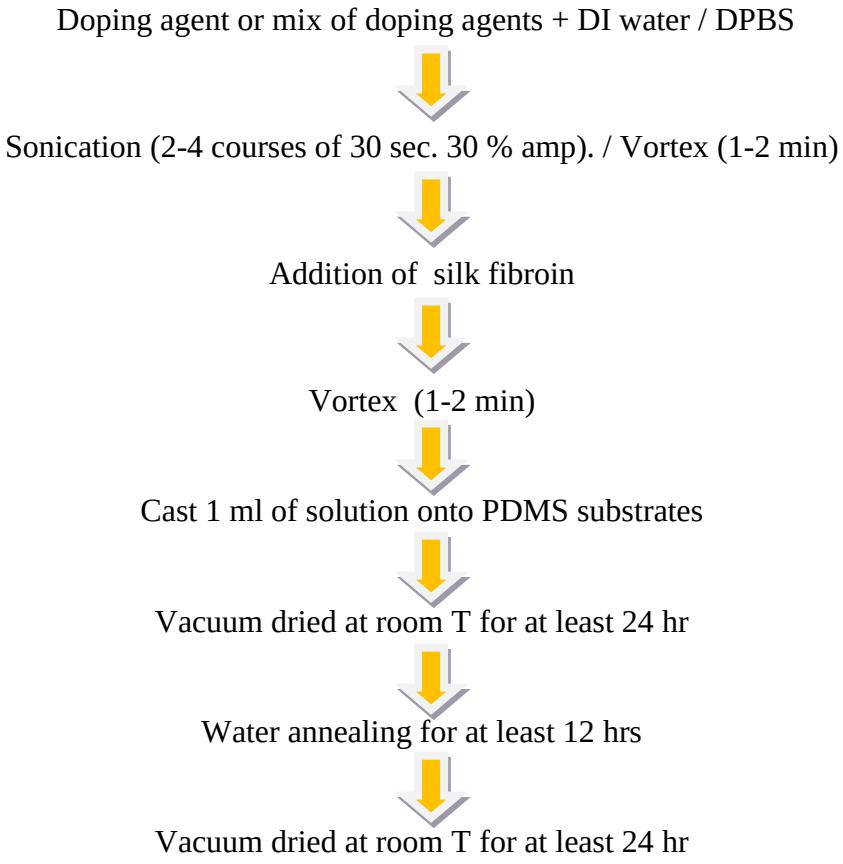

Figure 12. General protocol for blending silk fibroin with dopants.

In all cases, the dopants were first added into a 15 ml falcon tube that contained water and were then vortexed for 1-2 minutes or sonicated for 2-3 courses of 30 sec. with 30 % amplitude. Afterwards, silk fibroin solution was added along with other additives such as glycerol or PEO. Solution was vortexed again for 1-2 minutes and then with the use of 1 ml pipette the films were cast on the PDMS and let dry overnight under the hood.

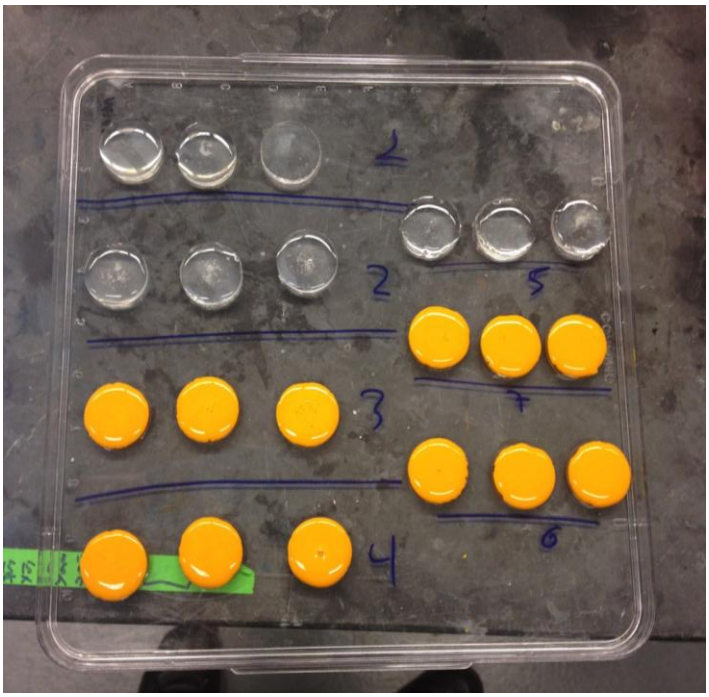

Figure 13. Representative picture of freshly casted solutions on 25.5 mm PDMS molds in triplets of 7 different conditions. The yellow color contain riboflavin as the doping agent whilst the transparent, NaCl.

3.2.3 Water annealing and methanol treatment

Water vapor annealing was imposed by placing the silk films to the isotemp vacuum oven (Figure 14), after they have been dried and peeled from the PDMS molds. The films are placed in petri dishes. Distilled water is also placed in the bottom of the chamber and the sealing is done with the use of a pump creating a vacuum approximately 23 in Hg. The water annealing process lasted 12 hrs [66].

The methanol treatment was also tried. The method includes the immersion of the films in 90 % methanol for 1 hr at room temperature.

After both treatments the films are placed again under the chemical hood with stable flow 0.2 m/s [62].

A B

Figure 14. A. The isotemp vacuum oven model 281A used for water annealing the silk films at 22 in Hg. B. Films taken out after water annealing.

3.2.4 Ultrasonic treatment

Sonication was used to troubleshoot the solubility of melanin due to the high granular surface morphology. Optimum concentrations, amplitude and time was adjusted to the Wang et al. paper [82]. The sonicator used was Branson Sonifier® Digital Cell Disruptor with 1/8" (3.175 mm) Tapped Horn, S-450D, 400W, 115V (Figure 29). The dopants compounds were diluted in the desired concentrations in water to a final volume of 5 ml in a 15 ml falcon tube. For all the blends the 2-4 courses of sonication were applied with 30 % amplitude.

3.2.5 Riboflavin with silk fibroin

Riboflavin was incorporated in silk films with the methodology described above. A wide range of concentrations was tried initially 2 % w/v, 5 % w/v and 10 % w/v. The protocol followed for these concentrations is presented in Figure 12. Higher concentrations ranging 10-40 % w/v were also applied along with the addition of glycerol ranging from 10-40 % w/v and 2-4 % w/v PEO.

3.2.6 Melanin with silk fibroin

Initially used concentrations of melanin were 0.05 % w/v, 0.5 % w/v and 5 % w/v. The protocol applied for these concentrations was the blending of melanin with silk fibroin. For higher concentrations ranging 4-10 % w/v of melanin sonication was applied for 3-4 courses of 30 sec. with 30 % amplitude. Moreover, NaOH was added to adjust the desired pH =10 of the solution. The composition of the films that contained NaOH was 4-10 % w/v melanin added to DI water or DPBS, 20 % w/v glycerol and 3 % w/v silk fibroin. The methodology of blending is as described in Figure 12 plus the addition of NaOH at the end.

3.2.7 Fe(0) solid powder with silk fibroin

To fabricate Fe-silk films, suggested amounts of Fe(0) powder used that would not be toxic for the human body by Recommended Dietary Allowances (RDAs) were applied within a range of 4-8 % w/v [65]. These amounts are translated to 40-80mg per 1ml of solution.

Films of silk and Fe were fabricated by adding Fe to de-ionized (DI) water or DPBS then sonicate for 4 courses of 30 sec. and 30 % amplitude. Fe was also blended with riboflavin with concentration ranging 4-10 % w/v for riboflavin and standard for 4 % w/v Fe.

The solution was prepared as the Fe solution alone with the only difference that riboflavin was added initially along with iron in DI water or DPBS and then sonicated.

3.2.8 Ferrofluids with silk fibroin

The ferrofluid was purchased from Ferro Tec (EMG 700 EMG series water-based ferrofluids). The specific ferrofluid has 5.8 % v/v magnetic particle concentration and it is composed of 1-4 % v/v magnetite, 7-27 % by volume water soluble dispersant and 69-92 % v/v water.

Second ferrofluid candidate solution was synthesized based on the work that was published by Ciobanu et al. [69]. 10 ml ferrous chloride tetrahydrate 2.595 g $FeCl_2 4H_2O$ and 40 ml ferric chloride hexahydrate (4.093 g $FeCl_3 6H_2O$) were added in 2M HCl. This mixture was dropped into 500 ml ammonia solution 0.7 M under stirring for about 30 min. Fe_3O_4 precipitates and with the use of a magnet was isolated and separated from the solution. The pH was adjusted using aqueous ammonia. The iron content (% wt) was determined by evaporation of 0.5 ml of the solution in 60 °C for 2 hours. Three different solutions were prepared with 1 % w/v, 2 % w/v and 3 % w/v concentration particles.

3.2.9 Horseradish peroxidase (HRP) with silk fibroin

The protocol for the fabrication of the films with Horseradish peroxidase (HRP) is taken from Partlow et. al [70] and is described below (Figure 15). It was applied for various concentrations of our dopants melanin, riboflavin and Fe powder and also blends of riboflavin and Fe for 1 ml films.

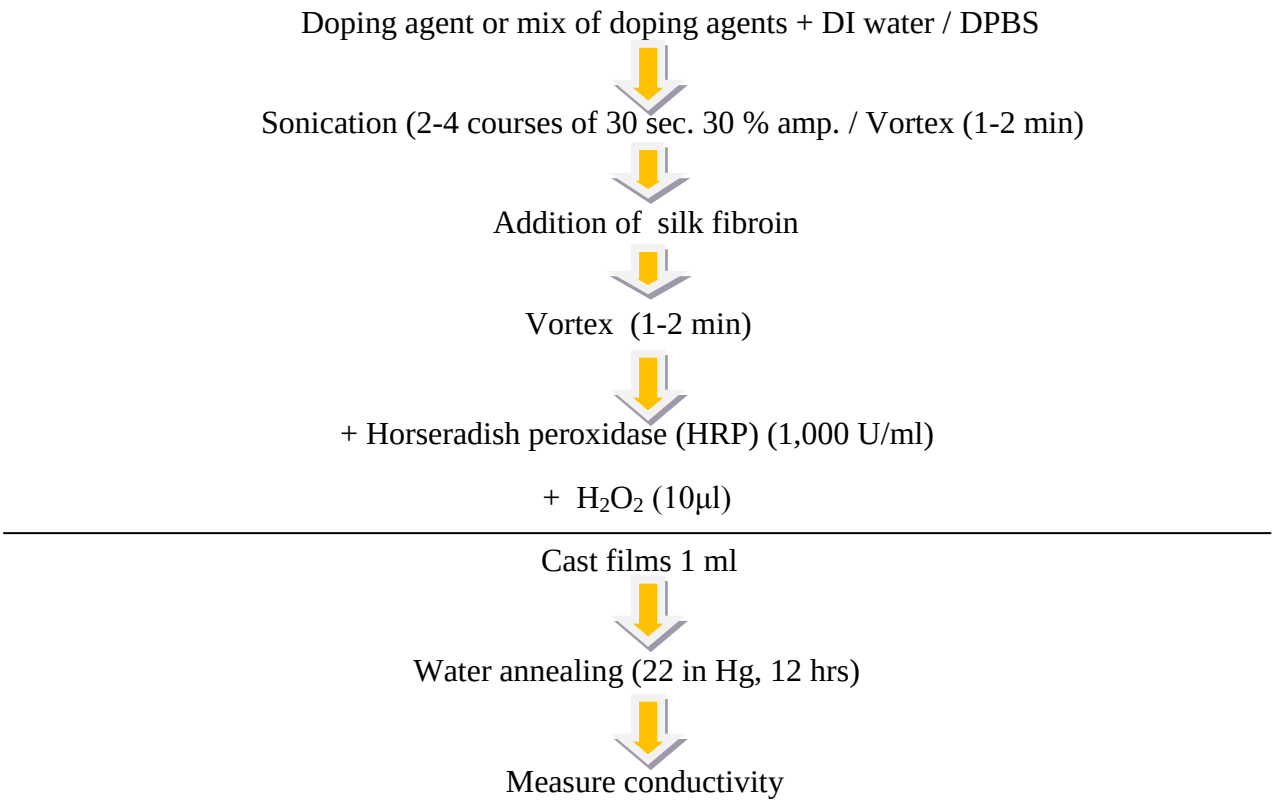

Figure 15. The protocol followed with the use of horseradish peroxidase.

3.3 3D Electroconductive scaffolds and incorporation of NaCl

In order to increase conductivity, procedure from Rockwood et. al. [2] was followed in the fabrication of water based NaCl-silk scaffolds. (Figure 16).

Figure 16. Description of the fabrication process of water-based silk sponges [2].

Three different sets of solutions were used. First set contains; 10 % w/v silk, 20 % w/v riboflavin, 30 % w/v glycerol, the second set contains 5 % w/v silk, 10 % w/v riboflavin, 10 % w/v glycerol and the third, 5% w/v silk, 20 % w/v riboflavin and 20 w/v % glycerol. The procedure continues by adding NaCl granules with sizes of 500 μm after they have been sieved with the appropriate sieves. For 2 ml of silk solution, 4 gr. of salt were used according to the protocol. After the addition of salt, the containers were placed in the oven at 60 °C for 2 hours. Scaffolds were placed in 4 lt beakers containing water for 48 hrs to remove the salt.

3.4 Silk melanin paper-like film

To prepare the melanin coated silk fibers the initial process is depicted in Figure 11. Initially, the *Bombyx-mori* silkworm cocoons were cut into small pieces approximately 2 mm side length. These small pieces of *Bombyx mori* silkworm cocoons were boiled in an aqueous solution containing 0.02 M Na_2CO_3 for 30 min. After boiling, the fibers were rinsed with distilled water to remove the sericin protein. Consequently, the fibers were collected and let to dry overnight.

To prepare the melanin films; 10 mg of melanin powder were dispersed in 20 ml of distilled water, to achieve good dilution and ultrasonic was applied for 2 courses of 30 sec. [2,71]. After that 50 mg of silk fibers were placed in the aqueous melanin solution and dispersed with the aid of mechanical stirring and ultrasonic. The ultrasonic was applied for 15 min in total with 15 courses of 1 min. After sonication the composite solution was filtered by a 5 cm diameter filter with 0.22 μm pore size under vacuum. The filtration lasted approximately 15 minutes and after that the composite film of melanin-silk fibers was dried at 65 °C for 2 hours. After 2 hours the film was unpeeled.

3.5 Spin coating thin silk film

Various concentrations of silk fibroin, riboflavin and glycerol blends were spin coated in order to produce a favorable film, that was both thin and formed well macroscopically. The concentrations of riboflavin and glycerol that were tested ranged between 10-30 % w/v while the concentrations of silk fibroin tried were 2-5 % w/v. The solution was prepared and described in Figure 12 with the only difference that the films were not cast but spin coated in glasses with size 24 x 50mm. Angular velocities tested ranged from 500 to 1500 rpm.

Different durations of spinning were tested, ranging from 10 seconds to 1 minute. The volumes of solution used were 1 ml. The spin coated film let to dry for 12 hours under chemical hood with 0.2 m/s air flow [76].

3.6 Electrospinning silk fiber mat

Various blends of doping agents along with silk fibroin solution were tried with the following concentrations; riboflavin ranging from 10-30 % w/v, silk 2-5 % w/v, PEO 1-3 % w/v and glycerol 10-30 % w/v with a final volume of 5 ml. Silk fibroin was first mixed with riboflavin and then PEO was added and vortexed for 1 min. Finally, glycerol was added and the blend was vortexed again for 1 min. The solution is loaded into a 5 ml syringe. The syringe was placed to a syringe pump with a speed of 0.5 ml/hr. They were two other parameters that were also adjusted in order to initiate a jet. One was the distance between the syringe and the collector which was 35 cm and the other was the voltage applied that was 20 keV. The blend that was able to form a film-like structure (Figure 45) consists of PEO 3 % w/v, 5 % w/v silk fibroin, 20 % w/v riboflavin and 20 % w/v glycerol.

3.7 The doctor blade (tape casting)

For the doctor blade method, a solution was made to be 5 % w/v silk fibroin, 20 % w/v glycerol, 30 % w/v riboflavin was used. The solution was vortexed and then with 1 ml pipette was cast along the blade (frame) onto the glass substrate with dimensions 20x30 cm and 0.5 cm thickness. The height of the blade was adjusted to 1 mm and the length of the blade was 10 cm.

The solution was spread with the doctor blade onto the surface of the substrate to form a uniform coating. After spreading the film it was placed under the chemical hood with 0.2 m/s air flow for 48 hrs to dry.

3.8 Measurement of silk film thickness

Measurements were performed with a Neiko 01407A Stainless Steel 6-Inch Digital Caliper with accuracy of 0.01 mm. The measurements were applied in two geometries to assess the differences in cross sectional areas between the center and the perimeter of the films. The round shape was preferred and used exclusively, because it was easier to create it with standard size PDMS molds.

3.9 The 2 point measurement technique for measurement of resistivity

With the 2 point method, current and voltage are measured in the same wire. The measured voltage is added with the potential difference created the wires (Ohms Law: V=RI). For values from 1MΩ/sq resistivity, this method can be used because contact and spreading resistance are negligible. For lower resistivity measurements, < 1kΩ/sq, this method will be not accurate because contact and spreading resistance will be very close to sample resistance (note that our resistivity measurements fluctuate, 0.1-0.5 MΩ) [73]. In the measurements, Keithley meter conductivity was used at a constant voltage of 2.1 V and 10 μA.

In the determination of resistivity, in order to reduce contact resistance between the electrodes and the film for the two terminals conductive paints at the electrodes rather than metal pressure contacts were used at room temperature (Figure 28).

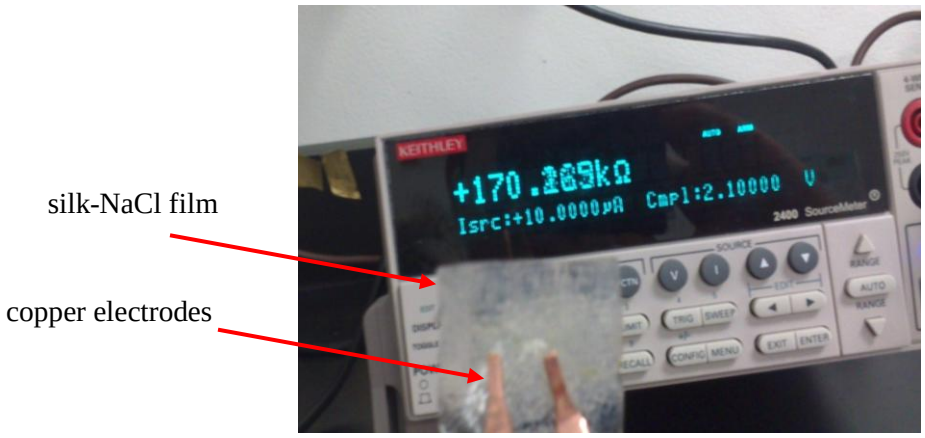

Figure 17. The Keithley's Series 2400 Source Measure Unit (SMU) and the measurement of the resistivity in one of the films.

3.10 Geometry of films and calculation of conductivity

To achieve accurate measurements of the films the geometry of the films should be considered.

The two point method is used to measure the resistance of the various films. To estimate the conductivity we need first to calculate the resistivity of each film, which is a different magnitude for each material.

The resistance of a disk is calculated by considering its geometry and the distance that the electrodes were placed.

For the disk of Figure 18, to calculate the resistance and thus the resistivity and find out how it is associated with the dimensions and the geometrical parameters, following equations were used. a is the radius, the thickness of the films is t ($t << a$) and also we define σ as the conductivity ($\sigma = 1/\rho$, ρ: resistivity).

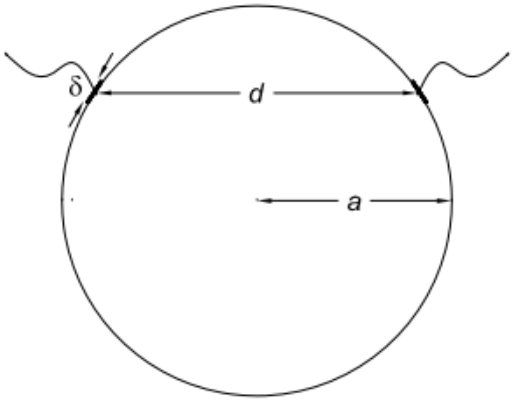

Figure 18. Disk geometrical parameters for conductivity measurements. a is the radius, d is the distance between the two measurement points and δ is width of the electrodes.

We define also δ, which is the width of the electrodes and d, the distance along the two points that the electrodes are placed to measure the resistance [74].

To derive step by step the formula which will give us the resistivity, Ohm's law R = V/I was considered. To estimate the 2 dimensional potential approximation of considering a cylinder of radius α with line charge λ that passes from the one contact and -λ that passes through the second contact was made for disks that measurement distance is more than δ/2 [74].

In the case of the a wire the electric field of charge density λ has magnitude in Gaussian Units

$$E_1 = 2\lambda / r_1 \quad (1)$$

according to Gauss' law where r_1 is the distance from the wire to the observer.

Then the electric potentional is $\varphi_1 = 2\lambda \ln r_1/r_0$ where r_0 is the constant of integration.

The potential due to the wire that has charge density -λ is similarly $\varphi_2 = -2\lambda \ln r_2/r_0$

r_2: is the distance from the wire 2 (second point of the measurement).

Then the potential at a random point will be

$$\varphi = \varphi_1 + \varphi_2 = 2\lambda \ln r_1/r_2. \quad (4)$$

Formula can be applied only for r_1 and r_2 that are greater than $\delta/2$ and that the potential for values that are smaller than r_1 and r_2 is constant. Approximation of the points (contacts of the electrodes) by perfectly conducting wires of radii $\delta/2$ is made (Figure 30).

The potential in contact 2 is estimated from (4) by setting

$$r_1 = d - \delta/2 \text{ and } r_2 = d - \delta/2.$$

Then

$$\varphi(\text{contact 2}) = 2\lambda \ln (d - \delta/2) / \delta/2 \approx 2\lambda \ln (2d/\delta) \quad (5)$$

To calculate the potential surface in contact 1 is the negative of (5), the potential will be

$$V \approx \varphi(\text{contact 2}) - \varphi(\text{contact 1}) = 2\lambda \ln 2d/\delta - (-2\lambda \ln 2d/\delta) = 4\lambda \ln 2\lambda/\delta \quad (6)$$

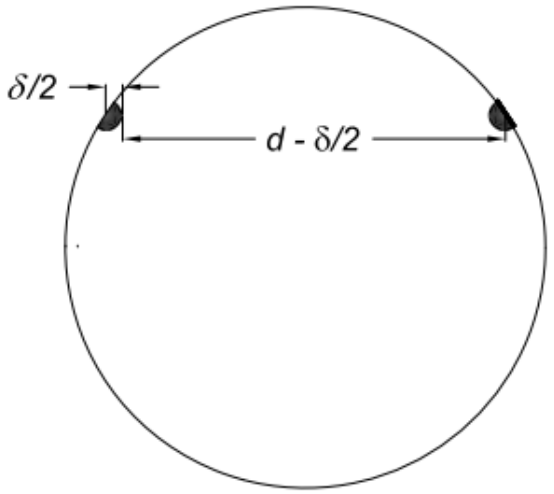

Figure 19. Approximation the contacts of width δ by perfectly conducting wires of radii δ/2, d>>δ.

At this point it should be noted that the electric field and current must be tangential to the edge of the disk. Also the equi-potentials described by equation 4 as well as the electric field lines that correspond to them are circles which pass through the line charges. This means that the boundary condition on the electric field is indeed satisfied.

Apart from the potentials the current is flowing needs to be calculated. The current, I, is given from the integral of current density J across any surface between two contacts.

To simplify; a cylindrical surface of radius r that is centered around of the contact and that is $\delta/2 < r , d$.

Since $r << d$, this surface is essentially an equipotential, and the electric field is essentially due to the nearby charge density λ. Namely, the electric field is normal to this surface, with magnitude

$$E= 2 \lambda/r \quad (7a)$$

For the current density that is $J = \sigma E$, in our case of a thin disc of thickness t, the relevant surface area is πrt and thus the total current is

$$I = \pi rt \, \sigma \, 2\lambda/ r = 2\pi\sigma\lambda t \text{ which is independent of r.} \quad (7b)$$

Substituting the equations (6) and (7b) in Ohm's law we will have

$$R = V/I = 4\lambda \ln 2d/\delta / 2\pi\sigma\lambda t = 2/\pi\sigma t \ln(2d/\delta)$$

that is independent of the radius of the disc.

From the last formula and since R is measured, solving for σ we have the conductivity of the material.

$$\mathbf{\sigma = 2 / \pi Rt \ln(2d/\delta) \quad (8)}$$

Concluding, to be able to calculate the conductivity, resistivity measurement with the Keithley meter, distance between the electrodes, the thickness of the films and also the width of the electrodes are needed.

3.11 Statistics

An initial screen of a wide range of samples was fabricated and tested with one sample per condition (Figures 53-55) to conclude to the best compositions and at the same time test the percentage of mass loss under specific treatments and conditions.

The optimized films (Table 8) were tested for mass loss and conductivity changes after water annealing with a sample size of n=6.

Error bars are shown as standard error of the mean. Statistical differences were calculated using students t-test. Statistical differences are show as * ($p<0.05$), ** ($p<0.01$), *** ($p<0.001$).

4. Results and Discussion

4.1 Melanin-silk films

In the beginning of the experiments various sizes and volumes of films were tried such as those in Figure 20, which depicts melanin-silk films of 100 μl volume and thickness of 1 mm.

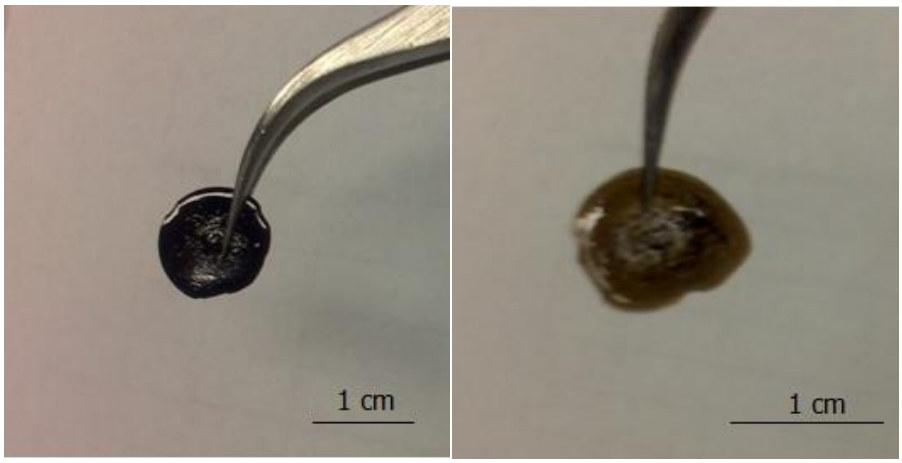

Figure 20. Two of the first films of melanin cast. They are made from the same tube containing 1ml solution. Each film is cast from 100 μl volume solution and the difference in color is due to different amounts of solute (melanin). Upper left film contains 0.5 % w/v, and the right one 0.05 % w/v.

As it is demonstrated in Figure 20 the first melanin-silk films did not have a uniform round shape and also contained a low amount of melanin. With higher concentrations of melanin, film formation was not successful due to the low solubility of melanin in water (2 mg/ml = 0.2 % w/v). Melanin powder consists of granules with various morphology and size distribution. Previous studies have shown that melanin for conductivity applications should be used in concentrations of 4-8 % w/v [38]. To tackle the low solubility of melanin, sonication was

applied. At the same time, for the sake of consistency, we optimized the sizes of the PDMS molds to 25.2 mm and the volumes of the silk blend solutions to 1 ml.

Sangram et al. [83] found the affect of the molecular weight (MW) of the silk solution was affected by the sonication conditions and tuned the MW in silk fibroin gels. Given their findings that the MW of silk fibroin decreased with sonication, our hypothesis was that with the application of sonication, melanin solution will increase the dispersion of melanin particles and cause lower stiffness in the films. Thus, sonication may help to overcome the brittle behavior and stiffness that the films exhibited.

A B C

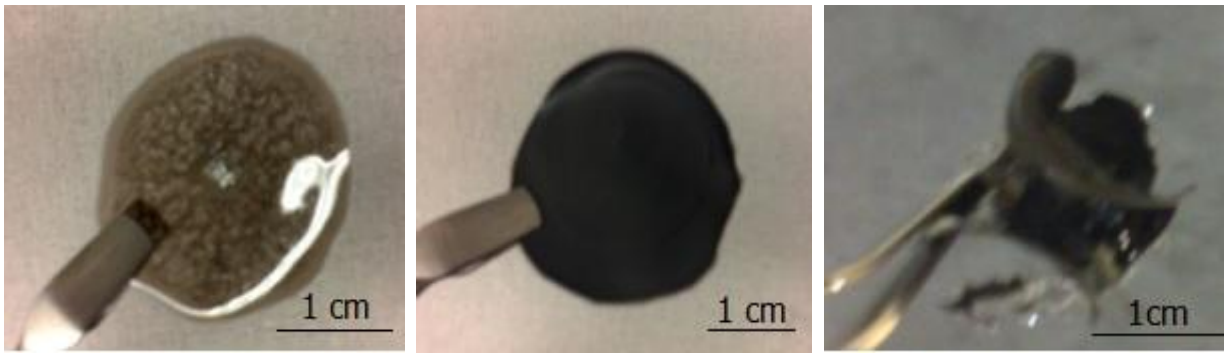

Figure 21. Silk-melanin films fabricated with aid of sonication with concentrations A. 0.05 % w/v, B. 0.5 % w/v and C. 5 % w/v. In film A the melanin granules are apparent and the low concentration of melanin results in no homogeneous dispersion of the granules. In film B there is good dispersion of the melanin. In high concentration of 5 % w/v, the films were shrunken and cracked.

The sonication made it feasible to form silk-melanin films at low concentrations of melanin. Moreover, the brittle behavior of the films was an issue. Our observations indicated that the increase of melanin concentration decreased the flexibility of the films. For the films presented in Figure 21, atomic force microscopy (AFM) was used to observe the morphology of films.

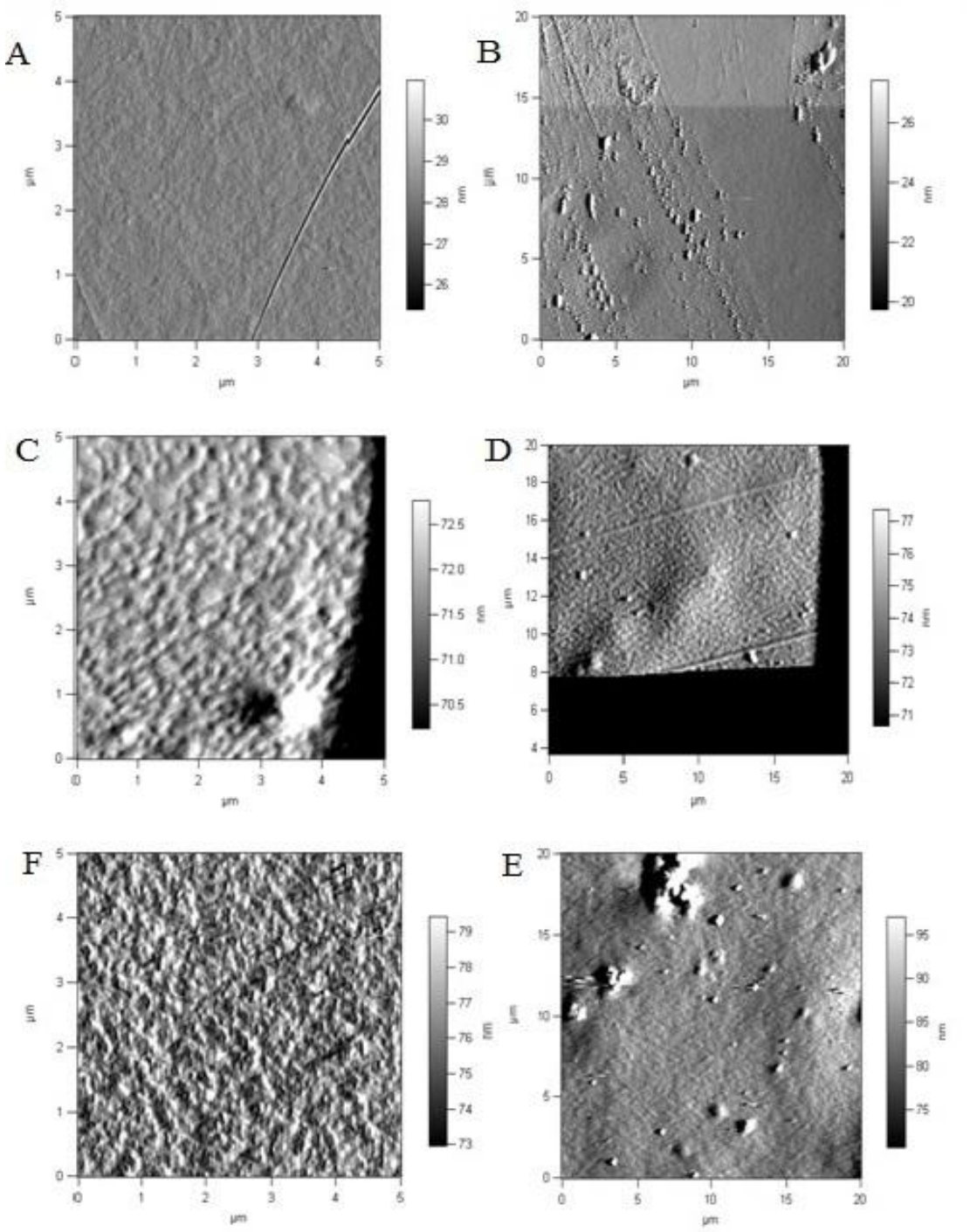

Figure 22. AFM images of silk-melanin films. Images were collected in contact mode and the deflection retraces are shown. A. silk fibroin 0.05 % w/v melanin, size of image 5x5 µm, scale bar of height 31 nm, B. zoom of image A, size of the image 20x20 µm, scale bar of height 26 nm, C. silk fibroin 0.5 % w/v melanin, size of image 5x5 µm scale bar of height 72.5 nm, D. zoom of image C, size 20 x 20 µm, scale bar height 77 nm, F. silk fibroin 5 % w/v melanin, size of image 5 x 5 µm, scale bar of height 79 nm, E. zoom of image F, 20x20 µm, scale bar height 95 nm.

AFM images are in accordance with the macroscopic observations. Specifically, for the films with 0.05 % w/v melanin, it is seen that the particles of melanin are dispersed and there are regions where they are absent due to the low concentration of melanin. For the films of 0.5 % w/v, the particles of melanin are dispersed in the film. Macroscopically, the film has a black homogeneous color. It is also obvious that the granules of the melanin vary in terms of size. The surface is not smooth, and it is wavy in some regions which indicates the brittle nature of the films. For the cracked film (Figure 21 C) with the highest concentration of melanin, the surface of the films looked rough and there is the formation of aggregates.

Resistance of the above mentioned films (Figure 21) was measured as described in Materials and Methods 3.9 and is presented below (Table 2).

Concentration of melanin	**Resistance (GΩ)**
0.05 % w/v (Figure 21 A)	300
0.5 % w/v (Figure 21 B)	100
5 % w/v (Figure 21 C)	Mechanical failure

Table 2. Resistance of the melanin-silk films presented in Figure 21.

As presented in Table 2, the formation of the films was achieved with the aid of sonication for low concentrations of melanin. Hence, the resistance of the films was high, falling into the insulator (conductivity < 10^{-7} S/m) category with given resistance values. The action of melanin is apparent since the increase of the concentration of melanin resulted in a decrease of resistance. Silk blends with 5 % w/v melanin concentration did not form any film so the resistivity was not measured.

In parallel with these blending experiments, Fischer esterification was tried, which was presented in Figure 9. The key difference of this protocol is the alteration of the pH to mild acidic conditions with the use of acetic acid (CH_3COOH). For pH ranging from 4-6 the formation of films was not successful. However, for pH values around 2, films formed even with higher concentrations of melanin up to 4 % w/v.

Melanin and silk blending were tried also in basic conditions as opposed to the acidic environment in Fisher esterification. With the use of sodium hydroxide (NaOH) and a pH of 10, films with higher concentrations of melanin, reaching 8 % w/v were cast successfully. At the same time, the use of glycerol in the blends reduced the brittle behavior of the films. However, out of many experiments tried with these specific conditions, the formation of films was not consistent.

A B

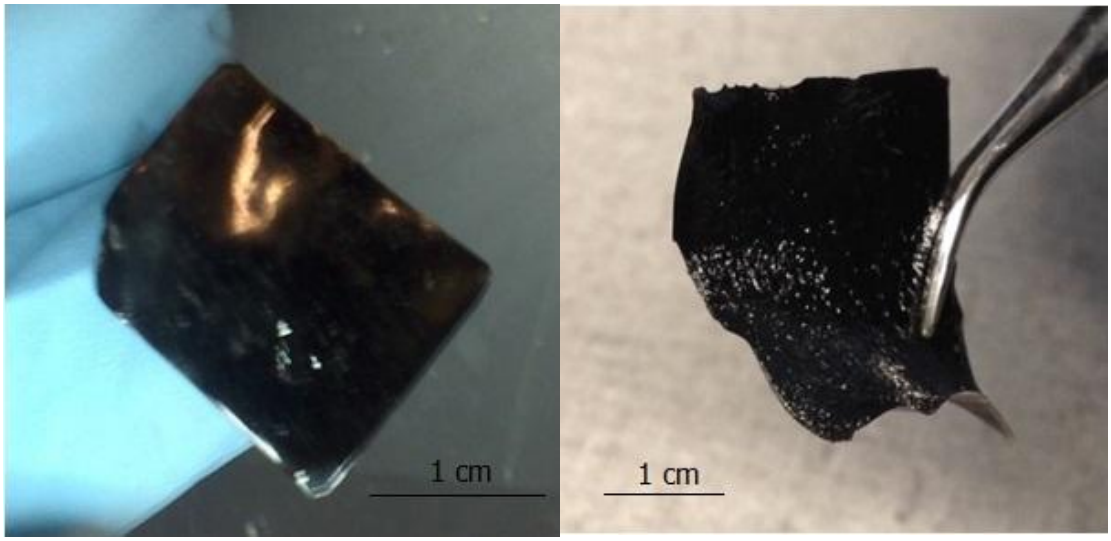

Figure 23. Melanin-silk films containing NaOH. On the left the film A contains 3 % w/v silk fibroin, 4 % w/v melanin and 10 % w/v glycerol. On the right the film B contains and 3 % w/v silk fibroin, 8 % w/v melanin, and 20 % w/v glycerol.

To tackle the problem of brittle behavior and low solubility, blending with glycerol in basic conditions was tried. The action and the benefits of glycerol were investigated better along with the riboflavin-silk films where it was easier to investigate with different concentrations due to high solubility and the easier reproducibility of the films.

A B

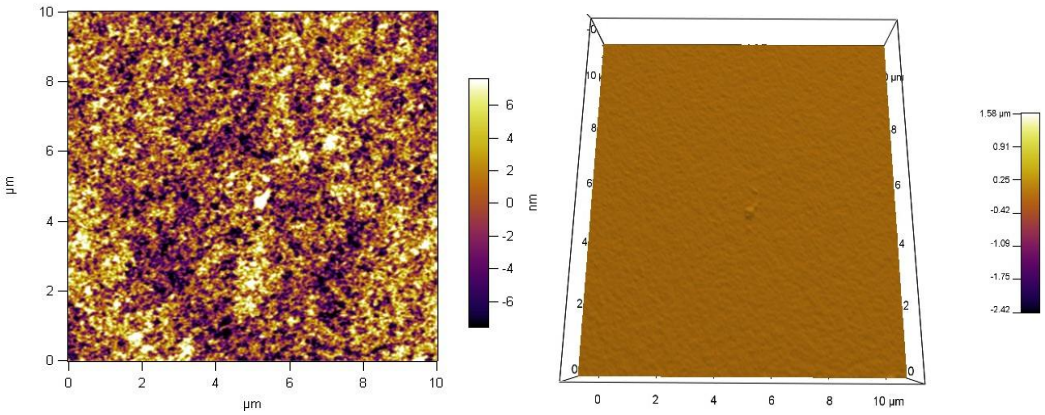

Figure 24. AFM images of Figure 23 with roughness measured R = 4.2 nm. Images were collected in contact mode and the deflection retraces are shown. A size of image 10x10 µm, scale bar of height 6 nm. B. 3D rendering of image A. size of image 10x10 µm, scale bar of height 1.56 µm.

As depicted in Figure 23 and confirmed by measurements of AFM in Figure 24, film A demonstrates a smooth polished surface. Doubling the amount of melanin causes a rough surface as is seen in Figure 23 B. Both of the films exhibited flexible behavior. In film B the amount of glycerol is double compared to film A.

Figure 25.The flexible behavior of the film containing 8 % w/v melanin.

As has been mentioned before, higher amounts of melanin cause more brittle behavior, therefore doubling the amount of glycerol resulted in less brittle behavior. It should be noted that when higher amounts of glycerol were incorporated with 8 % w/v melanin, the films exhibited flexible behavior (as could be seen in Figure 25) and vice versa. Basic conditions allow the use of high concentrations of melanin by increasing the solubility of melanin, and glycerol increases the flexibility of melanin-silk films.

Another method that was investigated to overcome the brittle behavior and fabricate films with homogeneous formation and good mechanical properties was based on the work of Partlow et al. [70] on covalently crosslinking silk via the catalytic action of horseradish peroxidase (HRP) and hydrogen peroxide on the tyrosine groups of silk (5 % of the total amino acids). With this method Partlow et al. managed to maintain the stiffness in silk hydrogels due to the β-sheet formation, while at the same time preserving the elasticity via the formation of the crosslinked silk hydrogels.

Silk hydrogels consist of hydrogen bonds and physical entanglements in the hydrophobic regions, and they result often in β-sheets. The unique β-sheet crystal structure of silk provides to these hydrogels good mechanical properties and gives the hydrogels stiffness.

The same HRP-silk blending ratios were used; however, the formation of films with HRP was not as successful as the hydrogels. The process we followed was to add the HRP and hydrogen peroxide after the sonication of the melanin in water. Upon addition of HRP, aggregation of melanin occurred making it difficult to cast films. The films also had a rough surface (Figure 26).

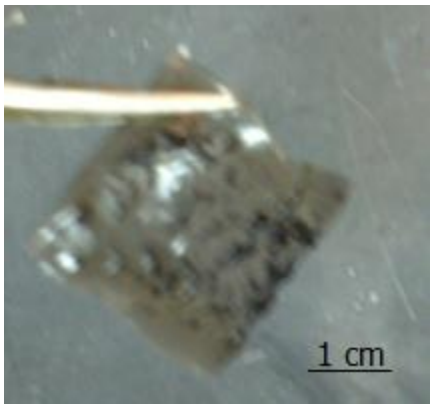

Figure 26. Melanin-silk film made with the HRP method. The melanin aggregates and low dispersion of the particles is apparent.

4.2 Melanin-silk paper-like sheets

One of the methods tried in order to overcome low solubility and improve the homogeneity of the melanin films was to create a paper-like film. Melanin is not well diluted in the silk fibroin, so this process could achieve a homogenous film by entrapping melanin molecules in the fibers of silk, creating a coating of melanin molecules absorbed or entrapped on the silk fibers.

Inspiration for this method is attributed to the work of Liang et al. [71] in which they showed that silk, an insulator, can be turned into a semiconductor by chemical reduction of graphene oxide on a fiber silk surface.

As is presented above, the formation of melanin-silk films was problematic and not reproducible mainly due to the low solubility of melanin powder which caused non uniform films. However, melanin films with semiconductive behavior were achieved, which indicated that silk and melanin could result in a useful semiconducting material. Following the method that Liang et al. [71] published in which they fabricated a flexible composite film of graphene and silk, the cotton like blackish mass of melanin-silk that is depicted in Figure 27 was created.

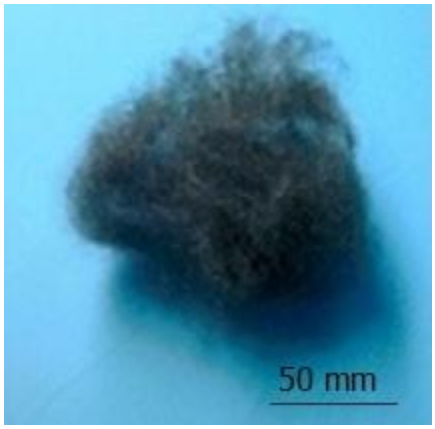

Figure 27. Melanin coated fibers after 15 min courses of sonication.

With the aid of a vacuum a composite paper-like film (Figure 28) was obtained. After unpeeling the paper-like film, the film was tested for conductivity. Our results with the Keithley meter indicated that the film was an insulator, with a resistance of 750 GΩ. We tried to coat melanin powder to silk fibers by sonicating the fibers in melanin aqueous solution in order to increase the melanin concentration. This technique has the advantage that high concentrations of melanin (> 10 % w/v) could be incorporated.

Given this advantage, this method could be an alternative to make electrically conductive silk fibers. An electroconductive paper-like silk-melanin film will have utility, with good mechanical properties, lightweight structure, flexibility, and chemical inertness.

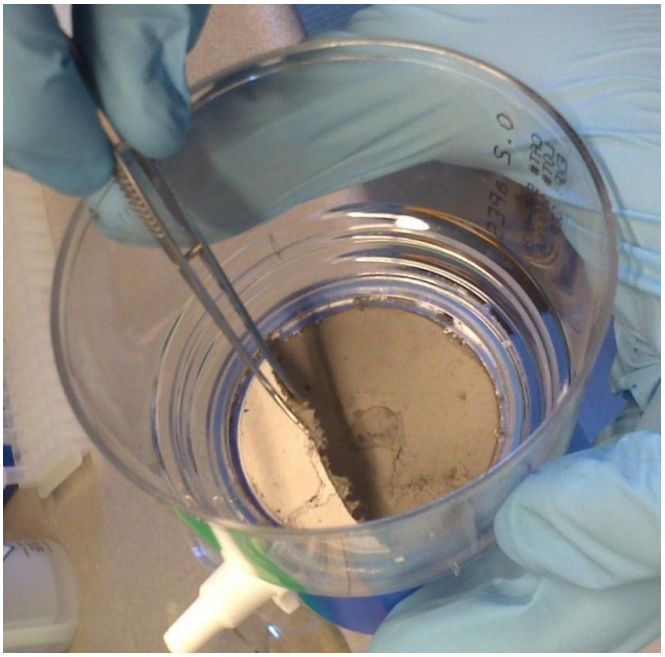

Figure 28. After drying at 65 °C for 2 h and peeling off the melanin-silk film from the filter.

4.3 Fe-silk films

Fe-silk films were made using the same concentrations as the melanin films 4 % w/v and 8 % w/v. The aim of this effort was to create a Fe-silk that is comparable in size to a commercially available nerve conduit for the repair of the ulnar nerve which has dimensions 8x20 mm, (a total area of 160 mm^2) [87]. For the fabrication of Fe-silk film with this area, 0.3 ml of solution were needed.

For the aforementioned iron concentrations, the amount of iron in 0.3 ml is equal to 12 and 24 mg. Commercially available nerve conduits have similar thicknesses and the total amount of Fe are not toxic even for acute intakes [65,88] that would occur if the film would completely dissolve, releasing the whole amount of iron.

A B

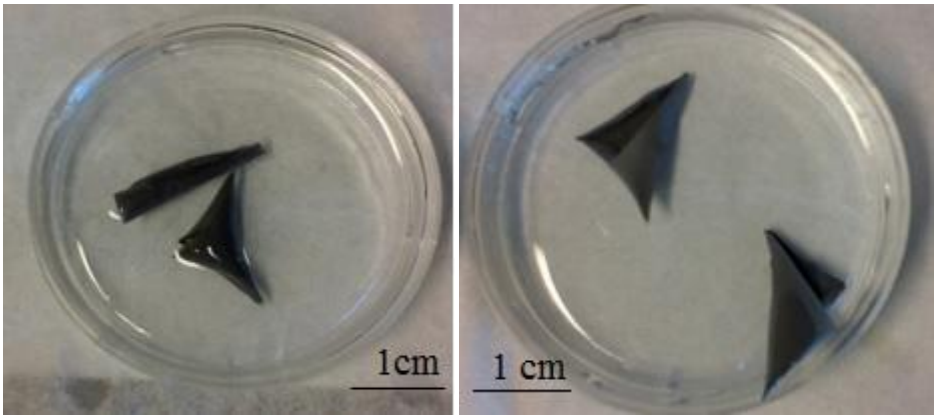

Figure 29. The first Fe-silk films: A. 5 % w/v silk fibroin, 4% w/v Fe. B. 5 % w/v silk fibroin, 8% w/v Fe. The films exhibited shrinkage.

Concentration of Fe	Resistance (GΩ)
4 % w/v (Figure 29 A)	1
8 % w/v (Figure 29 B)	0. 27

Table 3. Resistance of the Fe-silk films presented in Figure 29.

Fe-silk solutions were prepared comparably with melanin-silk solution concentrations that vary between 4-8 % w/v. Fe showed better solubility and dispersion than melanin which was insoluble in the aforementioned concentrations of melanin alone.

Considering the conductivity results and the ability to dissolve the iron powder in silk solution in concentrations of 4-8 % w/v, along with much lower values of resistance than melanin (100 GΩ), it can be deduced that iron powder can result in higher conductivities without solubility problems for concentrations of 4 % w/v. Moreover, the shrinkage that is depicted in Figure 29 can be overcome with the use of glycerol. However, it should be noted that for concentrations of 8 % w/v some debris was observed in the falcon tube if the solution was not cast within 1-2 minutes after blending.

4.4 Ferrofluid-silk films

The high conductivity results that were achieved with Fe-silk films triggered the application of other iron compounds such as ferrofluid. Ferrofluid, with its good dispersion of iron particles, would provide homogenous mixing with silk solution and result in a better texture and smoother surface than the Fe.

A B

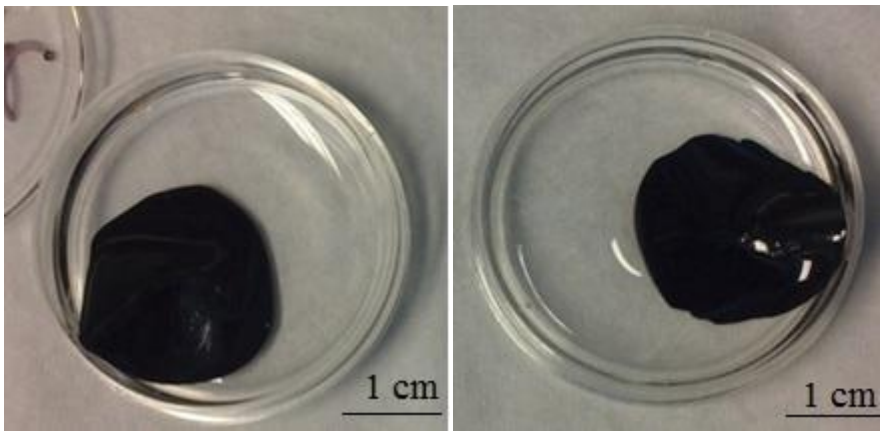

Figure 30. The ferrofluid-silk films. A. 5 % w/v silk fibroin, 1 % v/v ferrofluid. B. 5% w/v silk fibroin, 2% v/v ferrofluid.

Concentration of Ferrofluid	Resistance (MΩ)
1 % v/v	80
2 % v/v	90

Table 4. Resistance of the ferrofluid-silk films presented in Figure 30.

The results we acquired regarding the resistance of ferrofluid-silk films were 90 MΩ for 1% v/v concentration and 80 MΩ for the 2 % w/v concentration. Moreover, the films exhibited much more elastic behavior and a smoother surface. These results indicated that ferrofluid offers much higher conductivity than the Fe(0) powder (270 MΩ) at lower concentrations. The difference of 10 MΩ in resistance when the concentration was doubled can be explained by the saturation of the amount of ferrofluid. It should also be underlined that the ferrofluid provided flexibilty in the films without the use of glycerol.

4.4.1 Processing ferrofluid for use in silk films

The fact that ferrofluid resulted in higher conductivity directed us to seek alternative ways to prepare a ferrofluid that has been used in cells studies. Based on the study of Ciobanu et al. [69] the attempt was to synthesize the ferrofluid they created, test its conductivity and compare it with the commercially available one.The films fabricated with the processed ferrofluid exhibited conductivity of 200 GΩ. This value was lower than the resistance values of the iron powder (270 GΩ), possibly due to the better distribution of the iron particles (action of surfactant) as has been observed in the Fe-riboflavin blends in which iron precipitated on the bottom of the film. However, the conductivity results were not as good as compared to the commercially available ferrofluid.

It is possibly due to the fact that the processed ferrofluid contains lower concentrations of nanoparticles and/or nanoparticles with lower resistivity. Further investigation and tests with processed ferrofluids should be done along with cell studies that compare the cell viability between the melanin-silk blends and riboflavin-silk films.

4.5 The riboflavin-silk films

The first batches of riboflavin-silk films are presented in Figure 31. The films were brittle and cracked. The thickness of the films ranged from 1.1-1.4 mm.

A **B**

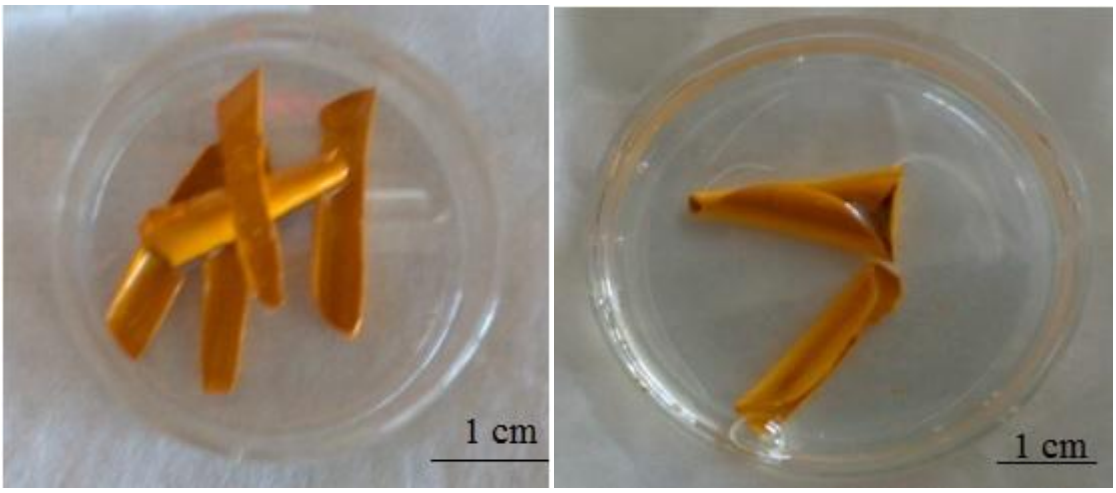

Figure 31.A. The early batches of riboflavin-silk films. A. 5 % w/v silk fibroin, 4 % w/v riboflavin. The films were fractured and broke into pieces exhibiting brittle behavior. B. 5 % w/v silk fibroin, 8 % w/v riboflavin. The films were brittle and shrunken.

Concentration of riboflavin	Resistance (MΩ)
4 % w/v	750
8 % w/v	450

Table 5. Resistance of the silk-riboflavin films presented in Figure 31.

The improvement of the casting technique and control of the thickness, along with the assistance of techniques such as sonication resulted in reduced resistance values down to 10 MΩ (Table 6).

A B C

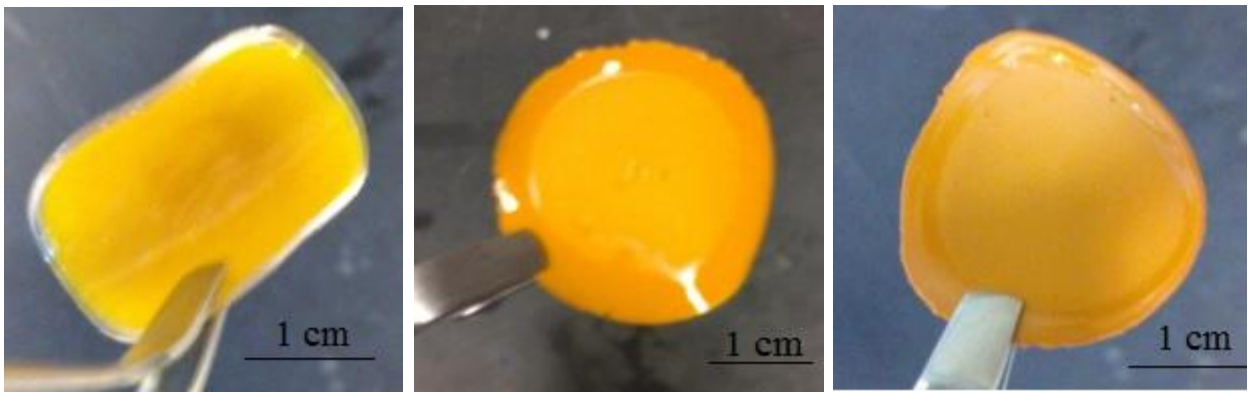

Figure 32. Riboflavin-silk films. A. 5 % w/v silk fibroin, 2 % w/v riboflavin. B. 5 % w/v silk fibroin, 5 % w/v riboflavin. C. 5 % w/v silk fibroin, 10 % w/v riboflavin.

Concentration of riboflavin	Resistance (MΩ)
2 % w/v (Figure 32 A)	20
5 % w/v (Figure 32 B)	10
10 % w/v (Figure 23 C)	10

Table 6. Resistance of the silk-riboflavin films presented in Figure 32.

As indicated in Table 6 there was a significant improvement of the homogeneous formation of the films, decrease in the thickness (0.5-0.7 mm) and thus elimination of resistance. Riboflavin exhibited the lowest resistance and consequently the best conductivity of all the compounds tried, achieving a resistance of 10 MΩ.

AFM was used to visualize the morphology of the films (Figure 33). AFM images demonstrated the uneven surface of film A with a concentration of 2 % w/v.

Compared to film B and C that had 5 % and 10 % w/v concentrations of riboflavin respectively, film A was more homogenous. The increase of riboflavin caused the formation of a rough surface. The increase of riboflavin concentration is apparent in the density and packed structure in film C. The smoother surface is depicted in the case of film B with the presence of some aggregates compared to film C.

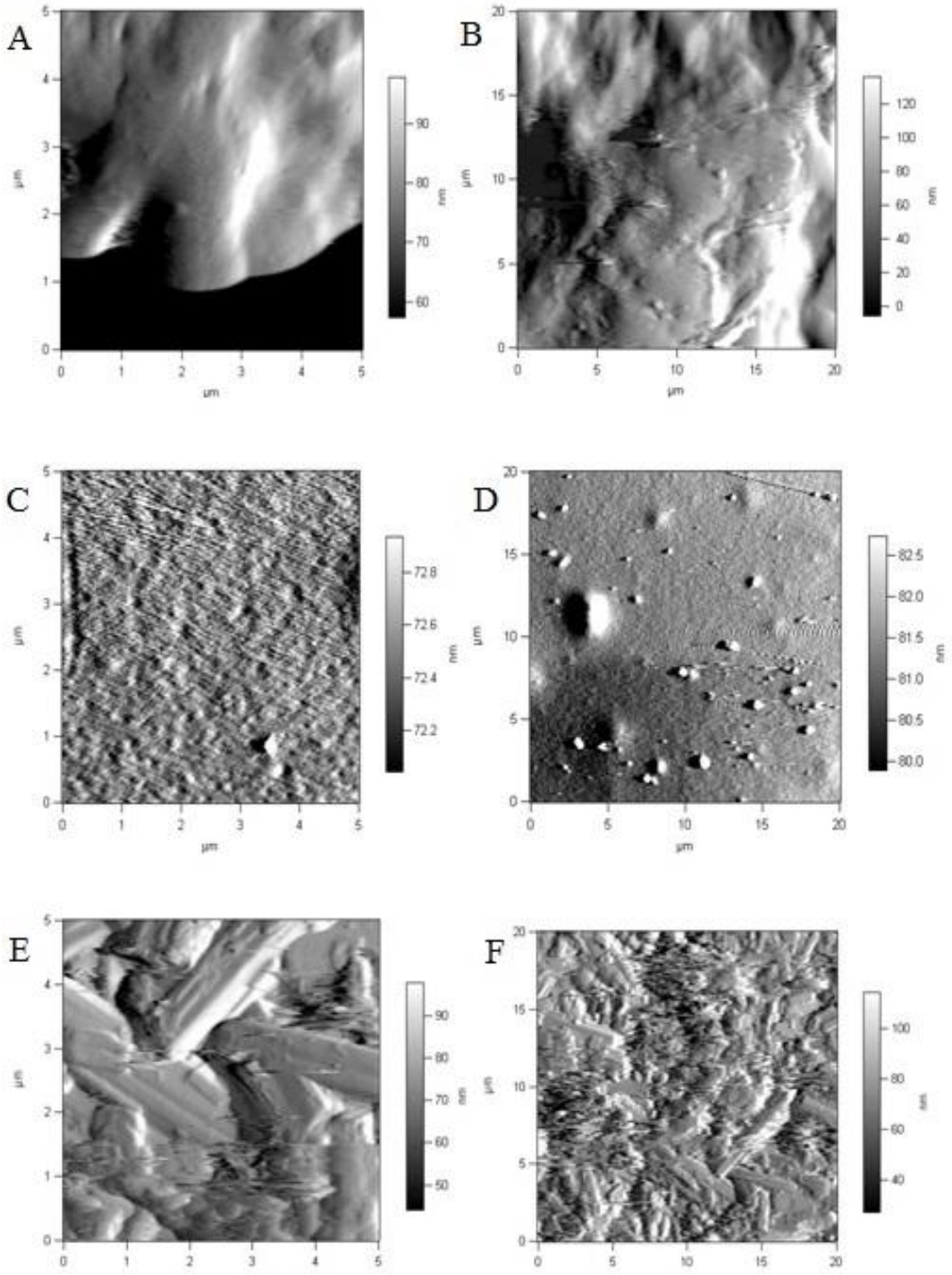

Figure 33. AFM images of riboflavin-silk films. Images were collected in contact mode and the deflection retraces are shown. A. 5 % w/v silk fibroin, 2 % w/v m riboflavin, size of image 5x5 µm, scale bar of height 90 nm, B. zoom of image A, size of the image 20 µm, scale bar of height 120 nm, C. 5 % w/v silk fibroin, 5 % w/v riboflavin, size of image 5x5 µm scale bar of height 72.8 nm, D. zoom of image C, size 20x20 µm, scale bar height 82.5 nm, E. 5 % w/v silk fibroin, 10 % w/v riboflavin, size of image 5x5 µm, scale bar of height 90 nm, F. zoom of image E, 20x20 µm, scale bar height 100 nm.

The values of resistance indicated that there was no difference when the concentration of riboflavin was doubled. A similar phenomenon was observed in the case of the ferrofluid, possibly due to the saturation of doping. The similar values of resistance might also be due to the crystal-like structures of the riboflavin molecules as shown in Figure 33 E. The effect of crystal structure in conductivity is discussed below, in the section of water annealing, where the formation of β-sheets in silk also resulted in differences in conductivity. This further reduction of resistance is depended on altering the concentration of silk, optimizing the sonication process (applying two courses of sonication for 30 sec. of 30 % power level) and also improving the casting technique. Moreover, the high solubility of riboflavin allowed the incorporation of a higher amount of the compound ranging from 10-30 % w/v, however this increase caused brittle behavior.

4.6 Glycerol effects on conductive silk films

Various amounts of glycerol were used and the results indicated that the addition of glycerol from 10-30 % w/v improved the elastic behavior of the films and at the same time increased the conductivity. With excess glycerol, especially in the riboflavin films, no film formation was observed, but a paste-like mass was formed (Figure 34) for concentration > 30 % w/v. We assumed that the simultaneous increase of riboflavin, in order to increase the conductivity, and of glycerol, in order to reduce the brittle behavior and contribute increased conductivity, could boost the conductive properties of the films. The experiments indicated that the results were irrelevant to the amount of riboflavin.

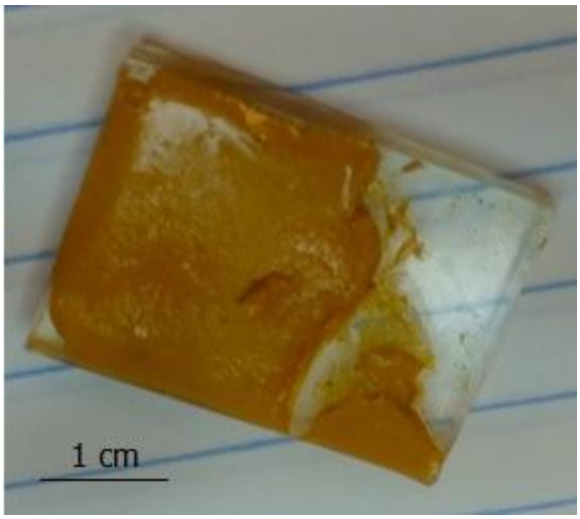

Figure 34. Paste like texture that occurs in higher than 30 % w/v concentrations of glycerol in riboflavin-silk solutions. Composition of film was: 5 % w/v silk, 20 % w/v riboflavin, 40 % w/v glycerol.

Glycerol improved the conductivity significantly thus confirming the results of Tsukada et al. [61]. In the case of Fe-riboflavin the resistance dropped more than 50 % for a 200 % increase of the glycerol concentration (Table 7). Moreover, a critical challenge was to control dissolution, and glycerol solved that problem. One of the main challenges for the implanted biocompatible films is retaining mass and function when exposed to an *in vivo*-like environment. Therefore, to test the durability of the films, they were placed for 7 days in PBS at 37 °C. Films that contained glycerol had enhanced durability and retained the shape and conductivity. Mass loss of the films ranged from 27-50 % (Figure 56) but films retained conductivity and exhibited lower flexibility. Our assumption is that the mass loss of the film blend corresponds to the mass loss of glycerol. Glycerol is very soluble in water and in alcohols [60].

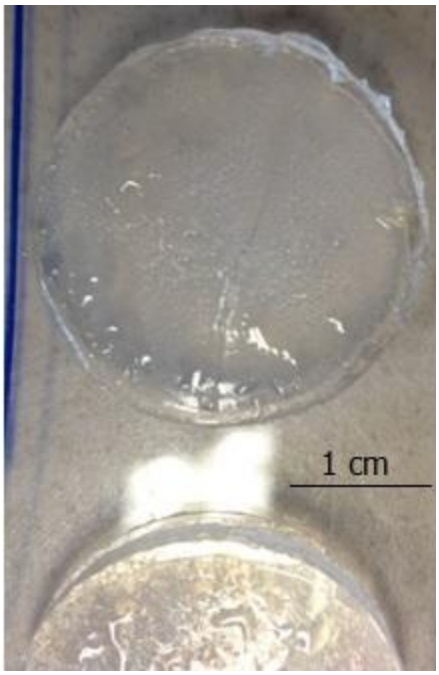

Figure 35. Elution of glycerol on the surface of the films.

This was observed in the first days on the drying films where elution of glycerol drops on the film surface occurred (Figure 35). After 7 days in PBS and 37 °C, the highest percentage of mass loss was due to glycerol loss. High leeching of riboflavin was not observed.

Glycerol increases the conductivity and integrity of the films. Therefore, high mass loss of glycerol in *in vivo* environments is a critical issue that affects the function and the integrity of the films.

4.7 Fe-riboflavin-silk films

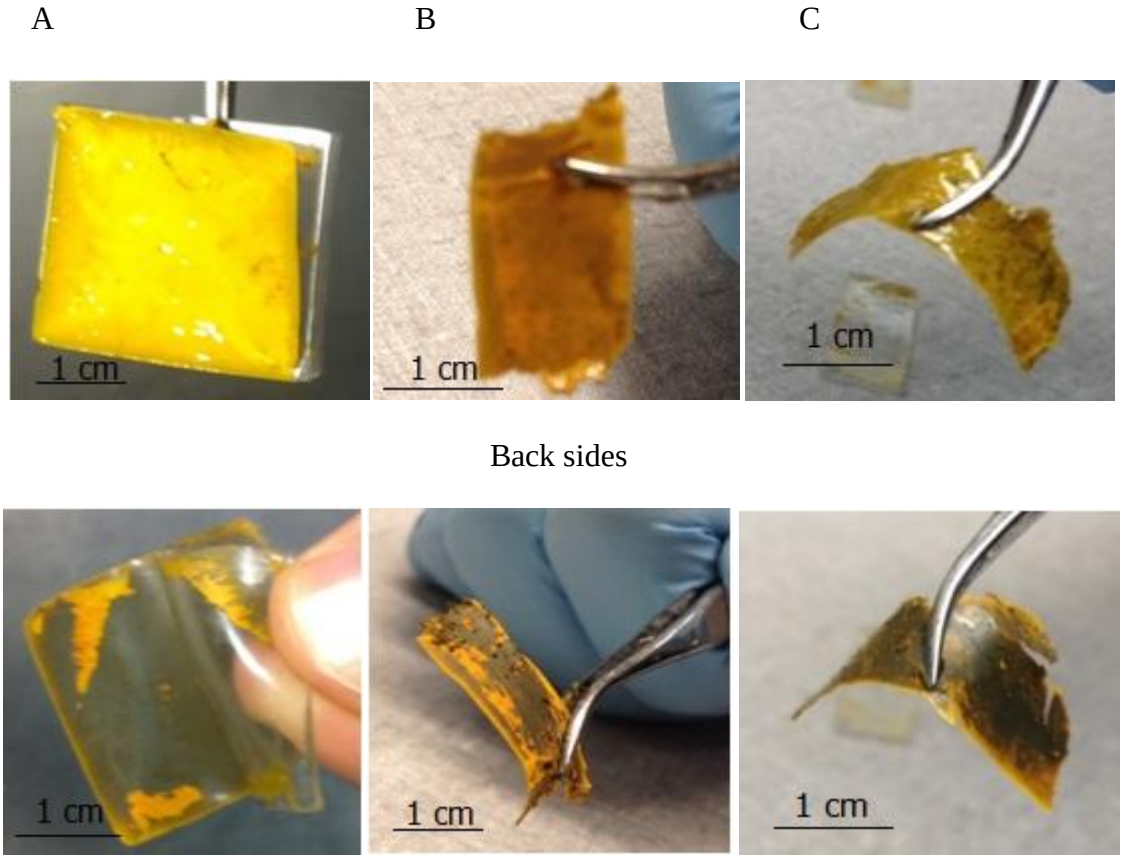

Figure 36. Top row front side of films and bottom row respective back side of Fe-riboflavin silk films A. 5 % w/v silk fibroin, 4 % w/v Fe, 4 % w/v riboflavin, 10 % w/v glycerol. B. 5 % w/v silk fibroin, 4 % w/v Fe, 4 % w/v riboflavin, 20 % w/v glycerol. C. 5 % w /v silk fibroin, 4 % w/v Fe, 4 % w/v riboflavin, 30 % w/v glycerol.

Iron powder was blended with riboflavin in equal amounts (4 % w/v) altering the concentration of glycerol (Figure 36). The higher concentration of glycerol resulted in films with poor mechanical properties and very thin films. The fact that films were thinner might indicate that the concentration of silk was too low. Thinner films are beneficial in terms of conductivity since from equation (8) we can see that when the thickness decreases the conductivity (σ) increases. However, in the case of the films in Figure 36, the resistance was higher than in the case of riboflavin alone. Moreover, the texture of the films were poor and easily cracked.

Iron powder aggregated especially in the case of film C. Another observation is the formation of a lower layer in the bottom of film A which indicates precipitation of iron whether the riboflavin is on the surface of the film (yellow color on surface, grey color on the bottom). The blends of Fe and riboflavin exhibited higher resistance than riboflavin-silk films therefore, the focus was on optimizing riboflavin films.

Glycerol Concentration	Resistance (MΩ)
10 % w/v	50
20 % w/v	35
30 % w/v	23

Table 7. Resistance of Fe-riboflavin powder for different concentrations of glycerol.

.

4.8 The HRP effect on silk films

The method of Partlow et al. was followed; in the riboflavin-silk films this method was applied and they exhibited resistance around 50 MΩ, while at that time the riboflavin-silk films with the incorporated glycerol had resistance around 10 MΩ (Table 6). So, the results indicated that the addition of glycerol was superior for the riboflavin-silk films versus the HRP crosslinking.

The HRP enzymatic crosslinking was also tried in the case of Fe-riboflavin blends with the same conductivity results as the riboflavin-silk films. The films also exhibited elastic behavior, however , the iron turned brownish, indicating oxidation (Figure 38).

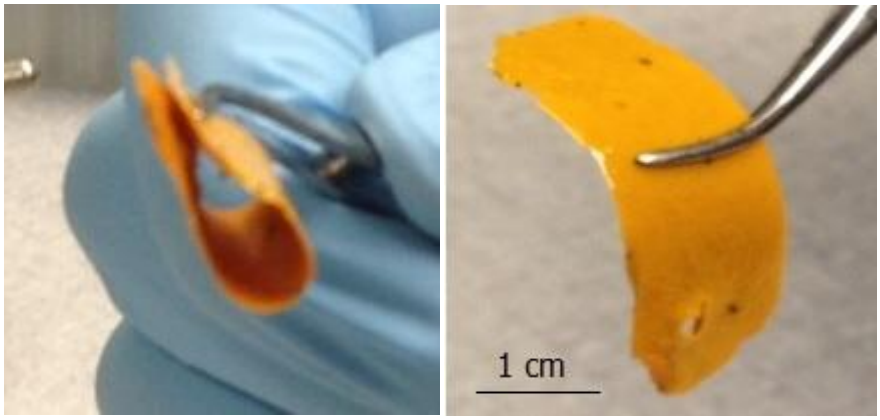

Figure 37. Elastic behavior of riboflavin-silk films due to action of HRP crosslinking.

This was due to the hydrogen peroxide in the reaction. These films also exhibited resistance varying from 20-50 MΩ for the same concentration of silk, riboflavin and iron (5 % w/v silk, 4 % w/v Fe, 4 % w/v riboflavin) which is comparable with the conductivity observed in the blend of Fe-riboflavin along with the addition of glycerol (Table 7). In this case, the glycerol and the HRP had similar results in terms of conductivity. However, between the two cases, there is a significant difference in the mechanical properties of the films. The addition of HRP caused the formation of a flexible film; yet, the precipitation of iron powder was still observed.

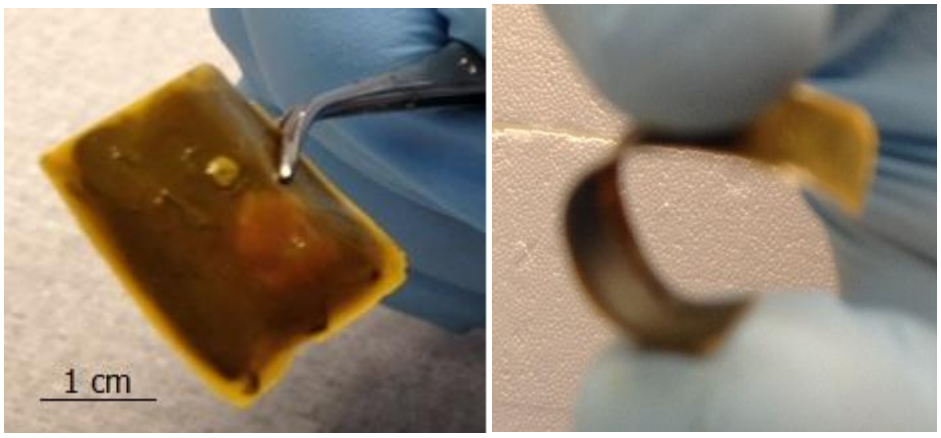

Figure 38. Fe-riboflavin silk films crosslinked with HRP. The elastic behavior is obvious along with brownish color of Fe oxidation due to H_2O_2.

4.9 3D Riboflavin salt leeched silk scaffolds

Salt-leeched silk scaffolds were fabricated with silk concentrations of 3-5 % w/v (Figure 39).

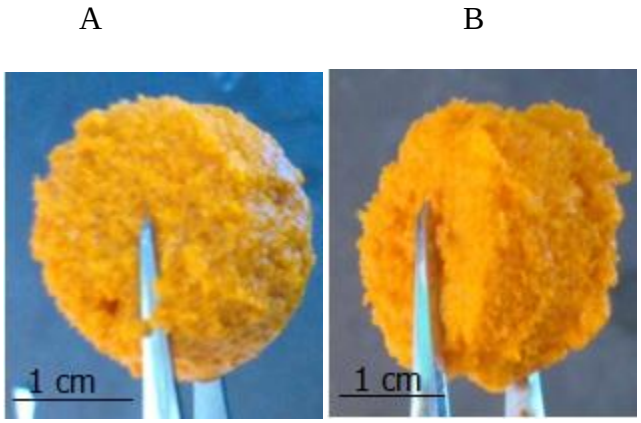

Figure 39. Electroconductive salt-leeched riboflavin-silk sponges. A. Composition of the sponge 10 % w/v silk fibroin, 20 % w/v riboflavin, 30 % w/v glycerol. B. 5 % w/v silk fibroin, 10 % w/v riboflavin, 10 % w/v glycerol.

The scaffolds exhibited resistance of 0.5 MΩ/cm. indicating that the combination of NaCl and riboflavin results in the low resistance. This finding led us to investigate the fabrication of films containing NaCl and riboflavin. Moreover, we investigated the mass loss of these scaffolds and the findings are presented in Figure 40.

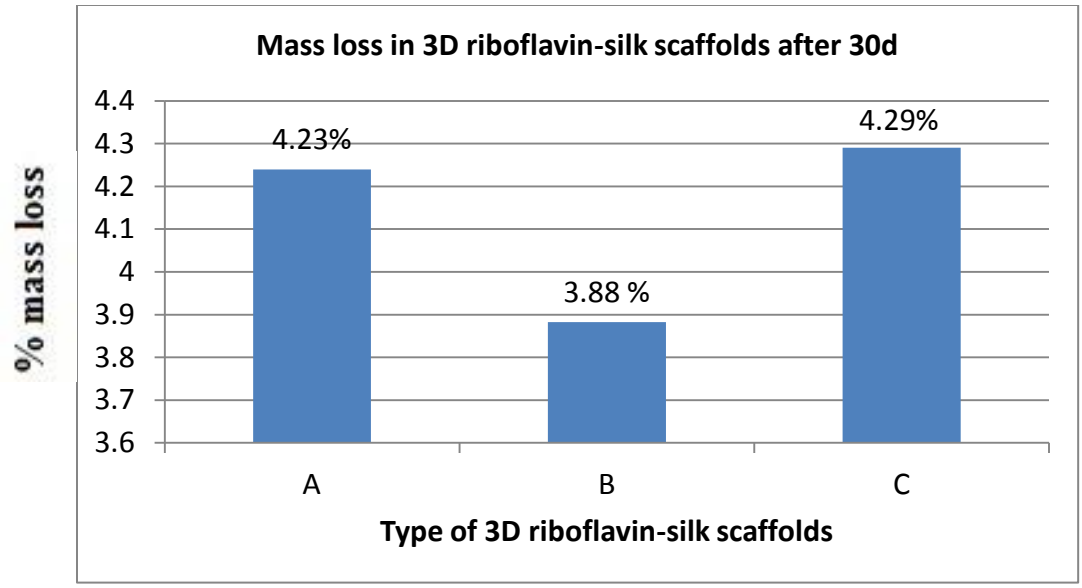

Figure 40. Percentage mass loss of 3D silk scaffolds after been 30 days immersed in 30 ml PBS in 37° C.

The composition of the films is as follows:

A. 10% w/v silk + 20% w/v riboflavin + 30 % w/v glycerol

B. 5% w/v silk + 10 % w/v riboflavin + 10 % w/v glycerol

C. 5% w/v silk + 20 % w/v riboflavin + 20 % w/v glycerol

Interestingly, the scaffolds exhibited low mass loss, and this finding directed us to investigate why this was occurring.

4.10 NaCl-silk films

A B

Figure 41. NaCl-silk films. A. 5 % w/v silk, 20 % w/v glycerol, 3% w/v NaCl. B. 5% w/v silk, 30 % w/v glycerol and 10 % w/v NaCl.

Formation of sodium chloride clusters is apparent in film A. Film B exhibited poor mechanical properties and cracked easily. The main difference that causes the integrity of film A is the rapid induction of β-sheet by placing the films in 60 °C. Film B exhibited high mass loss and rapid dissolution (it dissolved after 24 hrs, Figure 41 upper) once placed in aqueous solution due to dilution of the NaCl. This did not happen in film A, due to the treatment and rapid β-sheet induction. These films have another advantage which is transparency, which may be beneficial in applications where light interacts with the film.

4.11 Film formation with spin coating

Spin coating method is based on dissolving the polymer in a suitable solvent and depositing it on a rotating substrate. In spin coating the polymeric solution is placed in the center of the rotating disk (substrate). The adhesive forces at the interface liquid/substrate and the centrifugal forces exerted on the rotating liquid result in plating the solution on the substrate, through the radial flow. The spin of the disk at high velocities (e.g. 3,000 rpm) causes the solution to be spread across the surface [75]. The rotational speed and the viscosity of the solution mainly determine the film thickness. The faster the rotation, and the more dilute solution, the thinner the finished film. At the same time, evaporation of the solvent results in the increase density of the solution and thus in its viscosity. This creates a gradient concentration in the liquid film, which after evaporation of residual solvent entails the creation of a theoretically homogeneous and solid film[76].

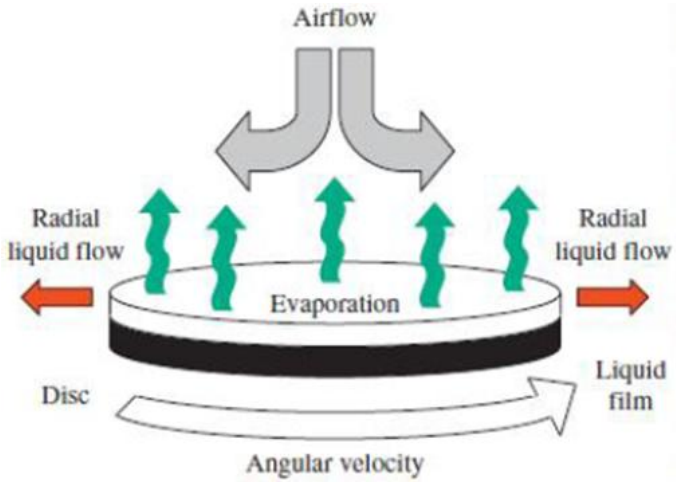

Figure 42. The phenomena of spin-coating [76].

The motivation of using the spin coating was its feasibility for fabricating thin films. According to formula (8) thin films result higher conductivity. Lowest concentrations of silk were desirable, since the thickness of the film affects its conductivity, with the thinner films being more conductive. Concentrations that were too low, 2-3 % w/v, inhibited the proper formation of a film, leaving only a liquidy solution. With the following concentrations of 5 % w/v silk fibroin, 10 % w/v riboflavin, 10 % w/v glycerol and angular velocity 1000 rpm and 20 seconds duration of casting, the best film in terms of morphology was cast.

The result is depicted in Figure 43. The biggest challenge was to peel off the film. At the same time, the values of resistance that were measured were much higher (100 GΩ) than the blending method (10 MΩ). The increased resistance may be attributed to uneven distribution of the riboflavin particles as is evident in Figure 43.

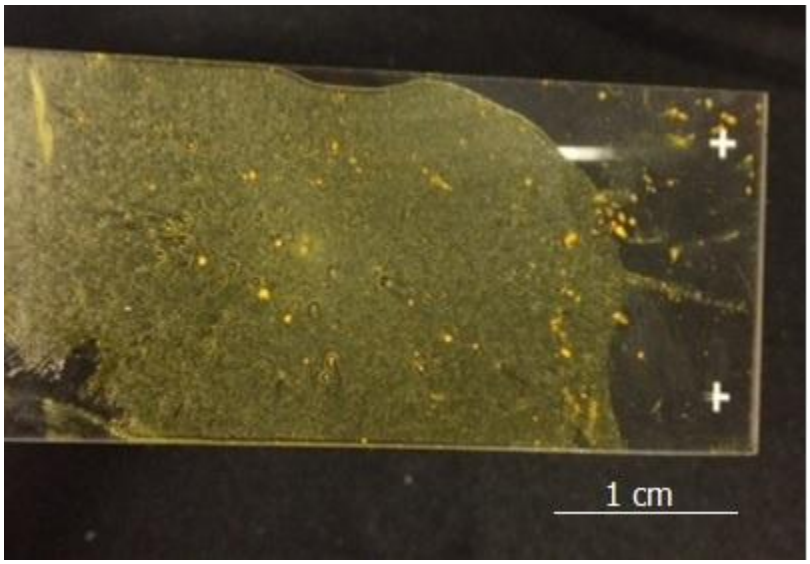

Figure 43. Riboflavin-films spin coated film. Riboflavin aggregates are apparent resulting the uneven distribution of the doping compound and thus not consistent conductivity over the mass of the film.

4.12 Silk fiber mat formation with electrospinning

In general, electrospinning is the method by which very fine fibers can be generated in the range of micro or nano from a solution, using a high voltage. The process does not require the use of high temperatures for producing solid fibers from solution [77].

This makes the process particularly suitable for producing fibers from high molecular weight molecules. When a sufficiently high voltage is applied to a liquid droplet, the electrostatic repulsion overcomes surface tension and droplet is stretched. At a critical point a quantity of liquid is ejected from the surface. This point is known as the Taylor cone. If the cohesion of liquid molecules is sufficient, then a jet charged liquid will be created.

.

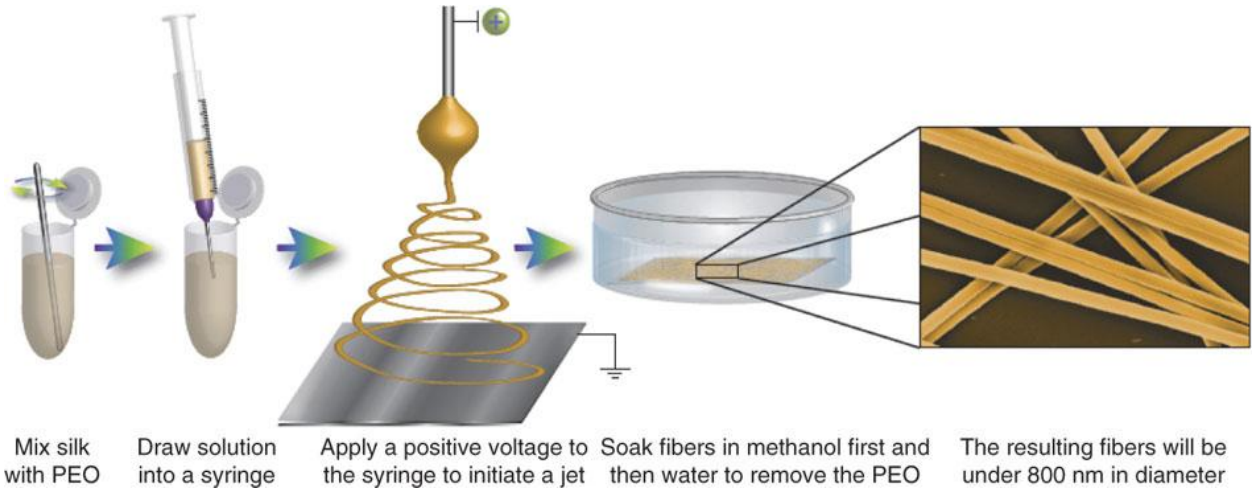

Figure 44. Process of fabrication of electrospun silk fibers [2].

The electrospinning device can be described as follows: a syringe mounted on a support to release the polymer at a constant speed and a constant voltage supply with continuous current is applied. A grounded collector of controlled distance (Figure 44) collects the electrospun fibers. [78,79].

The purpose of the experiment is to create a film with conductive properties and also explore the network and distribution of the dopant within the fiber mesh [78,79].

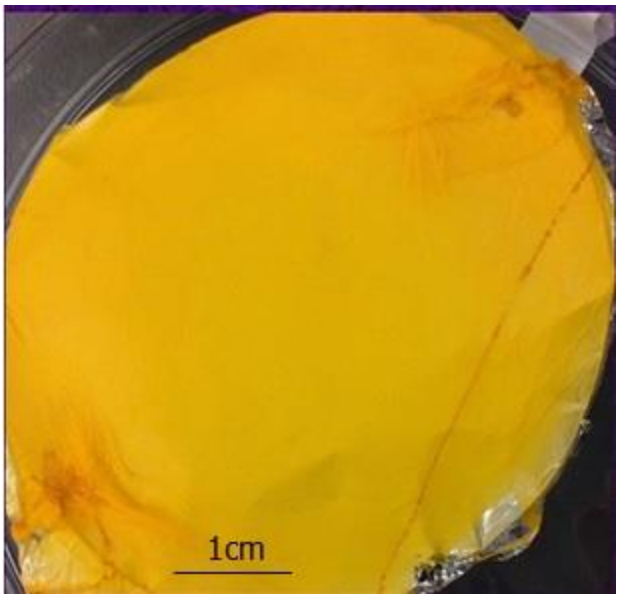

Figure 45. Macroscopic picture of the electrospun riboflavin-silk film. The film consists of PEO 3 % w/v, 5 % w/v silk fibroin, 20 % w/v riboflavin and 20 % w/v glycerol.

As seen in Figure 46, there are riboflavin aggregates in the fibers but not along the whole length of the fibers. Since the dopant here is riboflavin there is not continuous distribution and attachment of the regions in the fibers that contain riboflavin.

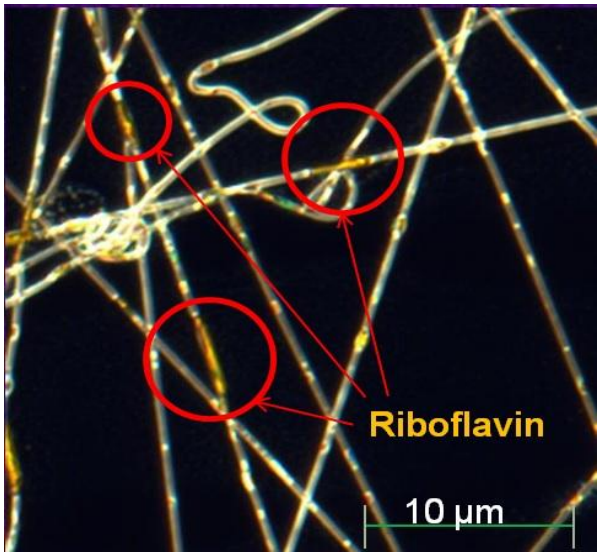

Figure 46. Phase-contrast image of the electrospun film that has been fabricated (Figure 45). The yellow aggregates depict the riboflavin.

To solve this issue, higher amounts of riboflavin should be used and also a much denser mesh of fibers to ensure the connection of conductive regions of the fibers. The low solubility of melanin along with the use of the viscous PEO solution limited its use.

4.13 Fabricating films with the doctor blades

Another method that is used widely for fabricating films on surfaces is the doctor blade. The technique was initially used and developed in the electronic materials industry for the production of thin films of capacitors and piezoelectric materials. Today it is considered a coating method. The doctor blade process is as follows: A suspension that contains particles and is well mixed along with other additives, for example binders, dispersants, diluents, plastisizers, polymerizing agents and is spread on a substrate (usually glass) by the doctor blade.

The doctor blade motion should be constant and the slurry solution is spread on the substrate creating a thin coating that can have different states and stiffnesses (gel or solid film). The doctor blade can be applied with a velocity of several meters per minute and can result in different thickness of a wet sheet (from 20 to several hundred μm) [80,81]. The regular doctor blade can also be used with a reservoir.

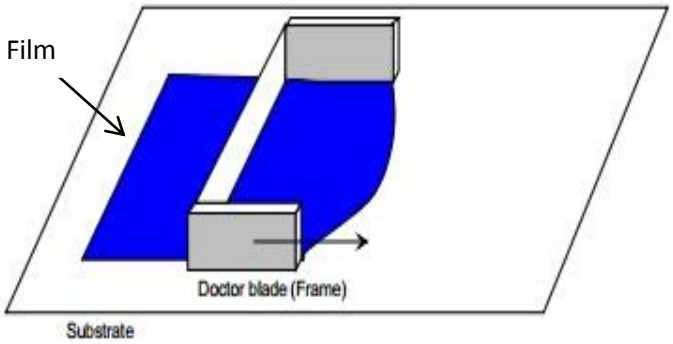

Figure 47. Doctor blading process, the coating liquid is spread onto the surface with the use of a frame which is moving relative to the substrate.

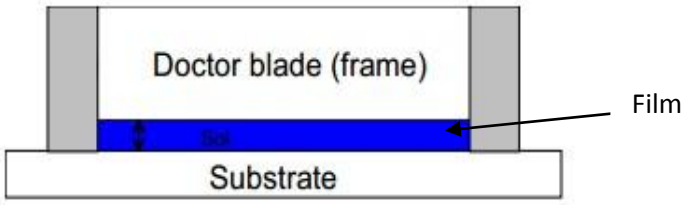

Figure 48. The thickness of the films can be controlled by adjusting the distance between the substrate and the doctor blade.

The thickness of the film depends on the geometry of the doctor blade and the properties of the coating solution, such as viscosity and the size of the dispersed particles. Theoretically, the thickness of layer is equal to the height of the blade from the substrate. Shear stress occurs in the solution during the layer application due to the surface tension of the suspension, its dynamic viscosity and the coating speed.

This results in approximately 20-30 % thinner films in practice against theoretical predictions. The thickness of the dried film also depends on the solid content and the density of the solution. Analytical models predicting the final thickness have been developed according to the aforementioned parameters [80,81].

The idea was to achieve uniformity and good dispersion of the granules of riboflavin. idea was to achieve uniformity and good dispersion of the granules of riboflavin. The low solubility and the higher size of melanin granules prevented the trial of the melanin-silk solution with this method.

Figure 49. One of the films that have been fabricated. The electrodes are placed to measure the conductivity of the spin coated riboflavin-silk film.

The rationale to apply this method was that the micro granules will be dragged and will be excluded from the coating. At the same time, it was hoped that the shear and friction applied to the solution and the granules dispersed in the solution will further will break down the riboflavin particles and result in higher uniformity and higher conductivity as well. Another plus of this method its simplicity and its quick formation of films (faster drying than regular casting techniques).

4.14 Optimization of blends for conductivity

As has been mentioned before, the two main obstacles to tackle are to increase the conductivity and to decrease the mass loss of the films. The compositions of the films that have shown better conductivity and were selected for optimization are presented in Table 8 below.

	Composition		**Composition**
Film 1	2 % w/v silk	**Film 4**	2 % w/v silk
	30 % v/v DPBS		40 % w/v DPBS
	20 % w/v glycerol		20 % w/v glycerol
	2 % w/v PEO		2 % w/v PEO
	48 % v/v H_2O		1 % w/v NaCl
			37 % v/v H_2O
Film 2	3 % w/v silk		
	10 % w/v riboflavin	**Film 5**	2 % w/v silk
	1 % w/v PEO		50 % v/v DPBS
	10 w/v % glycerol		10 % w/v glycerol
	30 % v/v DPBS		1 % w/v PEO
	37 % v/v H_2O		10 % w/v riboflavin
			1 % w/v NaCl
Film 3	2 % w/v silk		27 % v/v H_2O
	10 % v/v glycerol		
	10 % w/v riboflavin	**Film 6**	2 % w/v silk
	40 % w/v DPBS		40 % v/v DPBS
	20 % w/v PEO		20 % w/v glycerol
	3 % w/v NaCl		10 % w/v PEO
	15 % v/v H_2O		20 % w/v riboflavin
			8 % v/v H_2O
H_2O is included in silk solution		**Film 7**	5 % w/v silk
			65 % w/v H_2O
			20 % w/v glycerol
			10 % w/v NaCl

Table 8. Optimal film compositions with higher conductivity.

4.15 Effect of water annealing on conductivity

Part of the optimization process of the films (presented in Table 8) was the water annealing process. Water annealing contributed to further increase the conductivity as is presented in Figure 50.

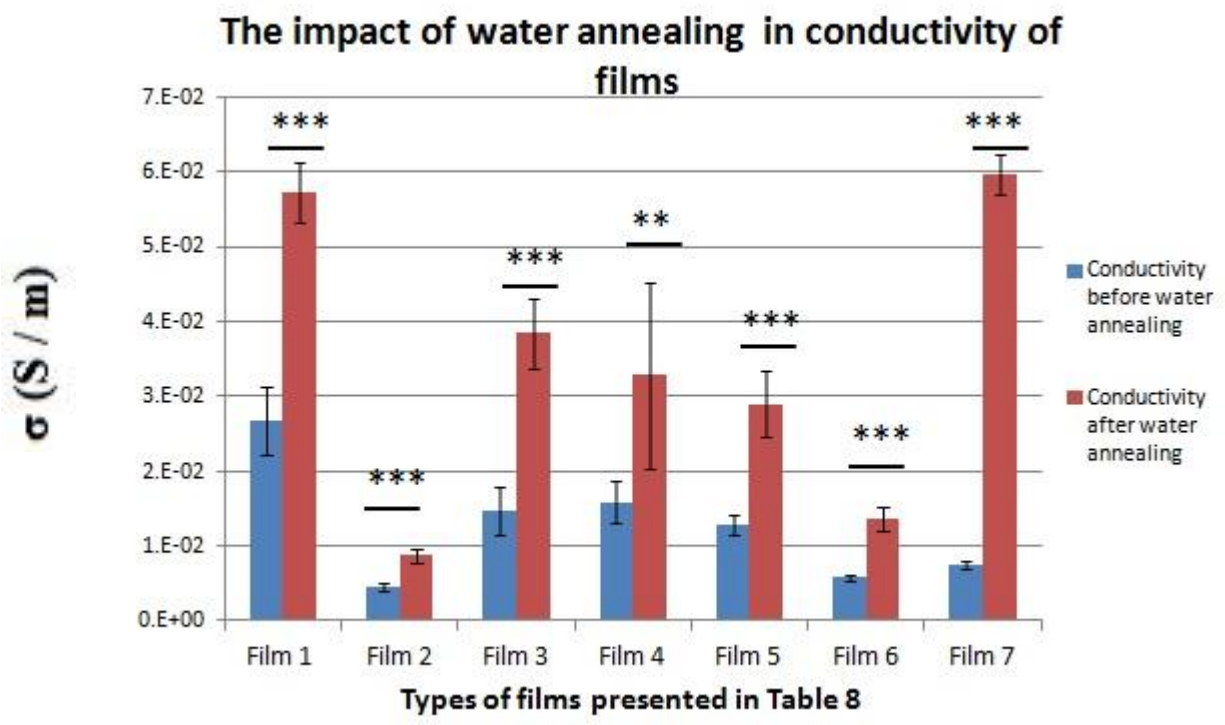

Figure 50. The effect of water annealing in conductivity of the 7 different film compositions selected for optimization. Sample size of n=6 for each composition. Water annealing (12 hr at 23 in Hg) statistically significant increase in the conductivity of all types of films. The highest increment was observed in Film 7 (indicates p<0.01, error bars = SE and *** indicates p<0.001, error bars = SE).**

Below there is an example of the calculations and the magnitudes for the films.

For Film 3 we measure Resistance R = 0.5 MΩ = 500.000 Ω, the thickness has been measured t = 0.0002 m, $\pi = 3.14$, $\delta = 0.0001$ m and d = 0.02 m solving for σ in formula 8,

we take $\sigma = 3.84*10^{-2}$ Ω/m which indicates according to Figure 54 that the film is classified as a semiconductor. The exact conductivities of the films of Table 8 are presented in Table 9.

It is apparent from these formulas that the conductivity depends on the geometry of the material. Therefore, the dimensions of the films that were fabricated were recorded. They were consistently cast of the same mass and on the same dimensions of molds, using the same electrodes and distance between the two points of calculations, which is 0.02 m.

Type of Film	Conductivity σ (S/m)
Film 1	0.0572
Film 2	0.0087
Film 3	0.0384
Film 4	0.0329
Film 5	0.0290
Film 6	0.0136
Film 7	0.0596

Table 9. Best achieved conductivities of the films of selected for optimization films (Table 8) after water annealing.

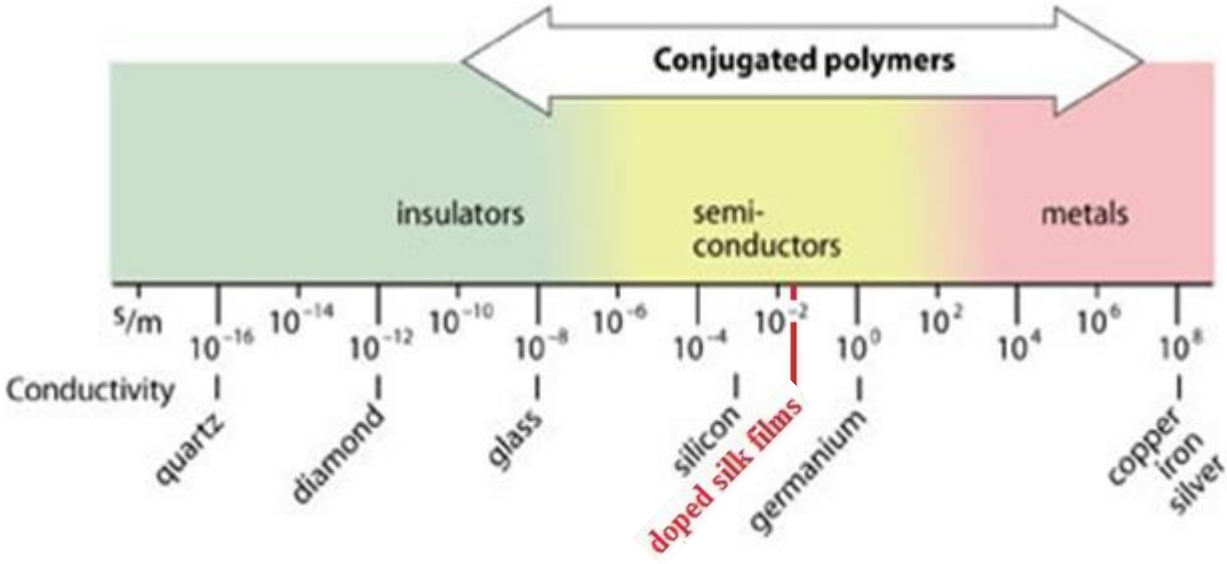

Figure 51. Conductivity of the optimized doped silk films (Table 9) in the range of conjugated polymers [18].

The increase of conductivity after water annealing can be explained as follows. Conductivity decreases when the chains are far away and increases if they come closer. Silk itself is not conductive because it does not have any charged residues or other weaker interactions such as Van der Waals or H-bonding. These minor interactions help in electron transfer. Silk has only C-C sigma bonds, which confines the electron in a defined location and does not facilitate transfer.

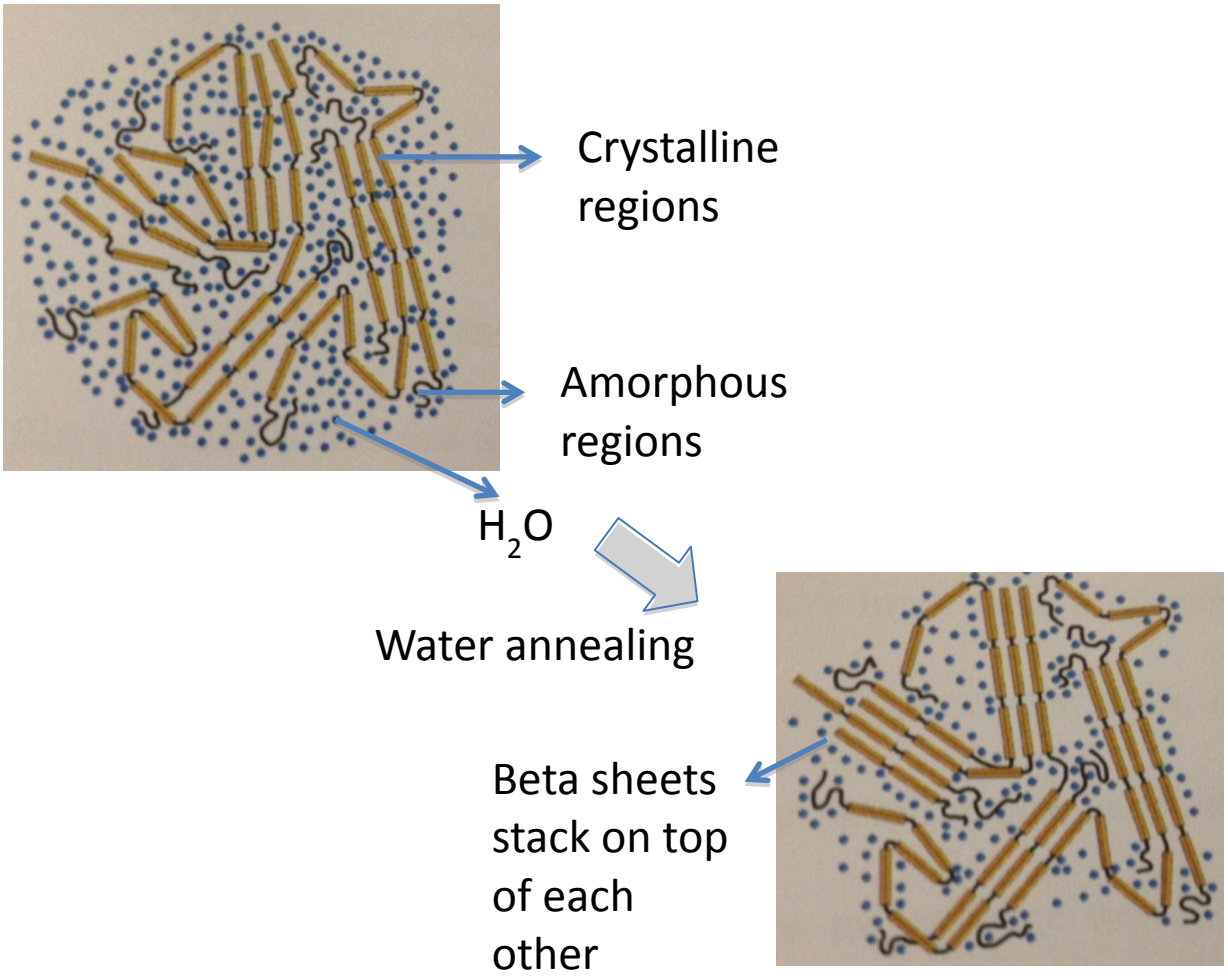

Figure 52. Effect of water annealing in silk fibroin chains [86].

Water annealing induces β-sheet formation that makes the overall structure more ordered and chains come closer via H-bonding. Not only do the chains come closer to increase conductivity, but they are also interconnected via H-bonding that facilitates electron transfer. β-sheet formation in silk via hydrophobic interactions is the key part for attracting riboflavin and melanin. Through hydrophobic interactions, π-π stacking and also minor H-bonding occurs. Riboflavin and melanin alone are conductors through their conjugated inner mechanisms. They facilitate the electron transfer as long as they are conjugated to the silk [86].

4.16 Effect of methanol treatment on mass loss and conductivity

Treatment with water vapor annealing and methanol have been found to impact the mass loss of the films and in the conductivity. Various films (Table 10) have been tested with one sample per condition in all cases. The results of methanol treatment are presented in Figure 53 and shown to increase the resistance and thus decrease the conductivity in all cases.

Film 1	**Film 2**	**Film 3**
2 % w/v silk fibroin	3 % w/v silk	3 % w/v silk
15 % w/v glycerol	30 % w/v glycerol	10 % w/v Fe
15 % w/v riboflavin	5 % w/v Fe	20 % w/v glycerol
50 % v/v HEPES	5 % w/v riboflavin	20 % w/v NaOH
18 % v/v H_2O	20 % v/v HEPES	30 % v/v HEPES
	37 % H_2O	17 % v/v H_2O
Film 4	**Film 5**	**Film 6**
5 % w/v silk	5 % w/v silk	3 % w/v silk
10 % w/v melanin	10 % w/v riboflavin	20 % w/v ribofavin
30 % w/v acetic acid	20 % v/v acetic acid	20 % w/v acetic acid
20 % w/v glycerol	30 % w/v glycerol	40 % w/v glycerol
35 % v/v H_2O	35 % v/v H_2O	17 % v/v H_2O
Film 7	**Film 8**	**Film 9**
5 % w/v silk	5 % w/v silk	5 % w/v silk
10 % w/v riboflavin	30 % v/v NaOH	30 % v/v HEPES
10 % w/v Fe	20 % w/v glycerol	20 % w/v glycerol
20 % w/v NaOH	45 % v/v H_2O	45 % v/v H_2O
20 % w/v glycerol		
35 % v/v H_2O		
Film 10	**Film 11**	**fillm 12**
5 % w/v silk	5 % w/v silk	3 % w/v silk
30 % v/v DPBS	10 % w/v NaCl	5 % w/v Nacl
20 % w/v glycerol	20 % w/v glycerol	30 % w/v glycerol
45 % v/v H_2O	65 % v/v H_2O	62 % v/v H_2O
Film 13	**Film 14**	**Film 15**
3 % w/v silk	5 % w/v silk	5 % w/v silk
4 % w/v melanin	10 % w/v riboflavin	8 % w/v Fe
50 % v/v HEPES	50 % v/v HEPES	30 % v/v HEPES
20 % w/v glycerol	20 % w/v glycerol	20 % w/v glycerol
HRP 1,000 U	15 % v/v H_2O	HRP 1,000 U
1 % v/v H_2O_2		1 % v/v H_2O_2
17 % v/v H_2O		30 % v/v H_2O

Table 10. Compositions of films that were tested for impact of methanol in their resistance (Figure 53), mass loss after been immersed for 1 hr in methanol (Figure 53) and mass loss after 7 days in PBS at 37 °C after been immersed for 1 hr in methanol (Figure 54).

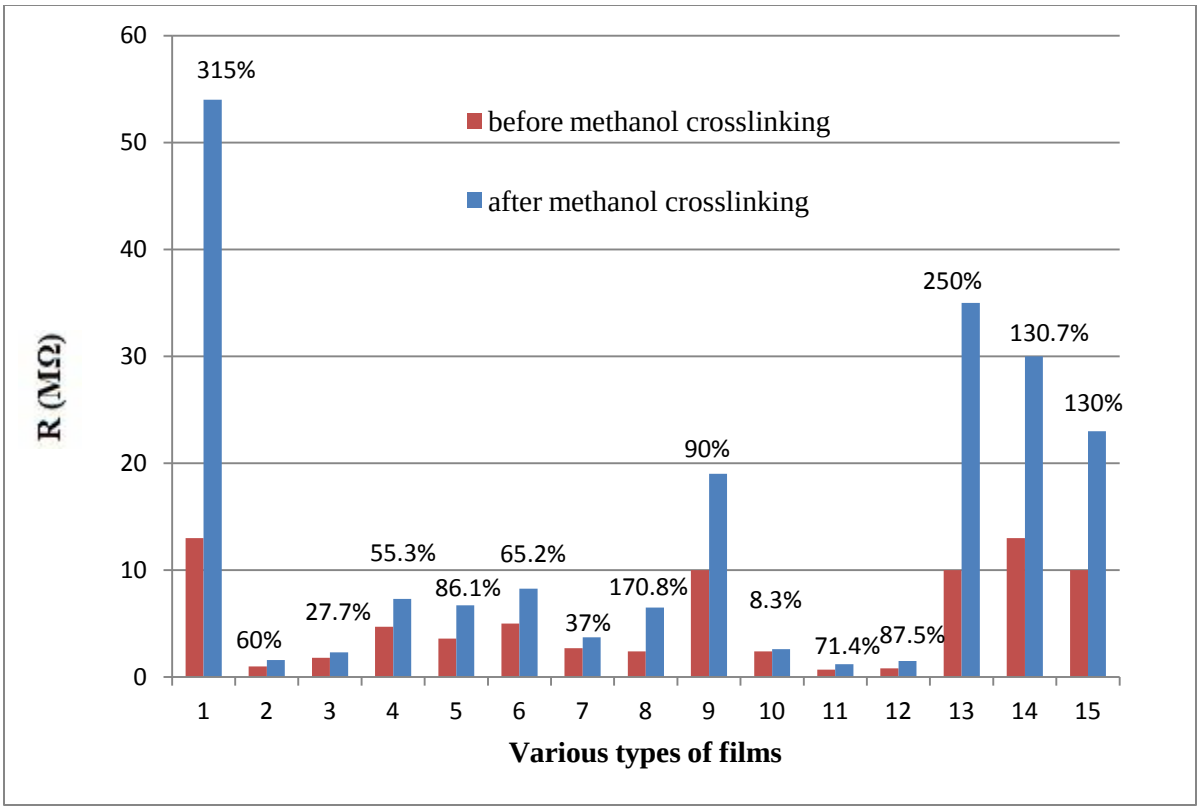

Figure 53. Impact of methanol treatment on film's resistance measured in MΩ. 15 different film compositions (Table 10) were tested with one sample per condition in all cases. In all cases it is observed significant increase of the resistance 250 % for film 13 and 130 % times for both 14 and 15 films.

Lawrence et al. have found that the thickness of silk films immersed in methanol increased 60 %, while the water annealing did not alter thickness [84]. Thus this increase of the thickness occurring after methanol treatment of the films increases the resistance. Mathematically, this can be explained with the formula we use to calculate the conductivity:

$$\sigma = 2/ \pi Rt \ln(2d/\delta)$$

when t is increased σ is decreased (or resistance is increased). The immersion in 90 % methanol might wash out glycerol in the films or the charge carriers that are contained in the blend due to the presence either of PBS or NaCl.

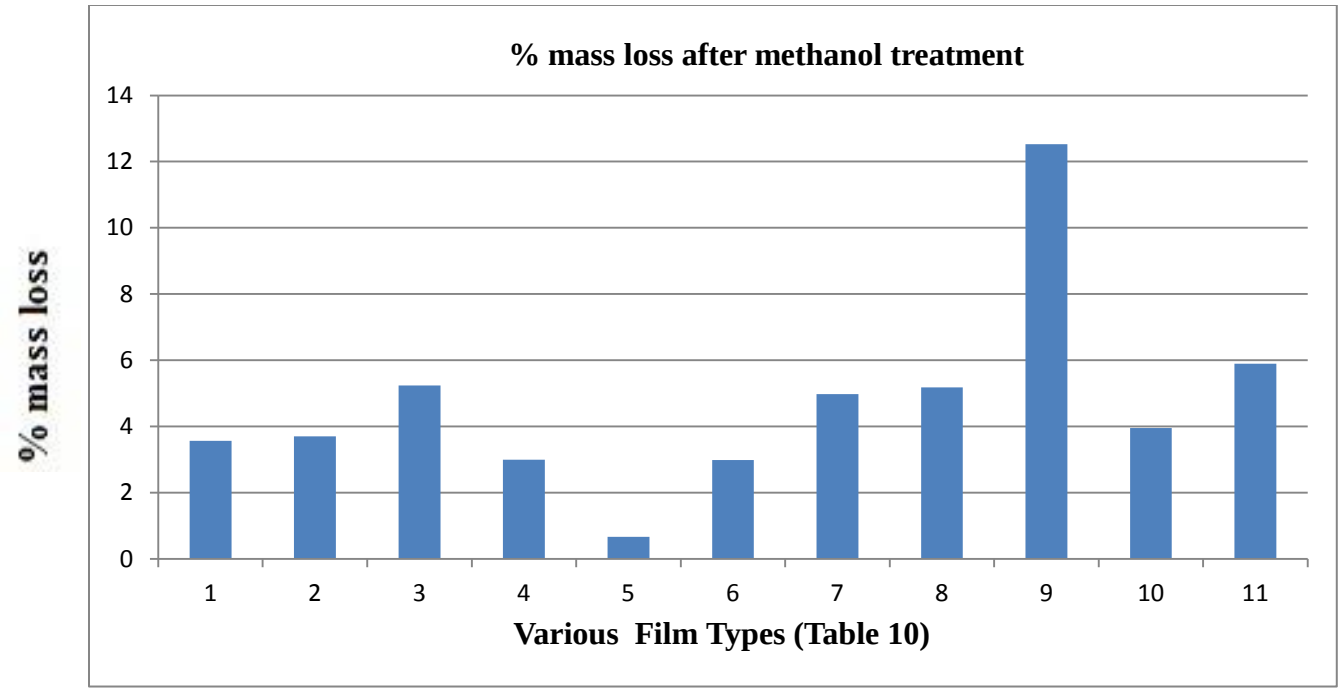

Figure 54. Percentage mass loss after been immersed for 1 hr in methanol. One sample per condition was tested in all cases.

We hypothesized that the immersion in 90 % methanol would wash out glycerol in the films or the charge carriers that are contained in the blend due to the presence either of PBS or NaCl.

The washing out of compounds is confirmed from Figure 54 and also from the data of Figure 55, where mass loss appears in all cases; this mass loss had significant impact on the conductivity (Figure 53).

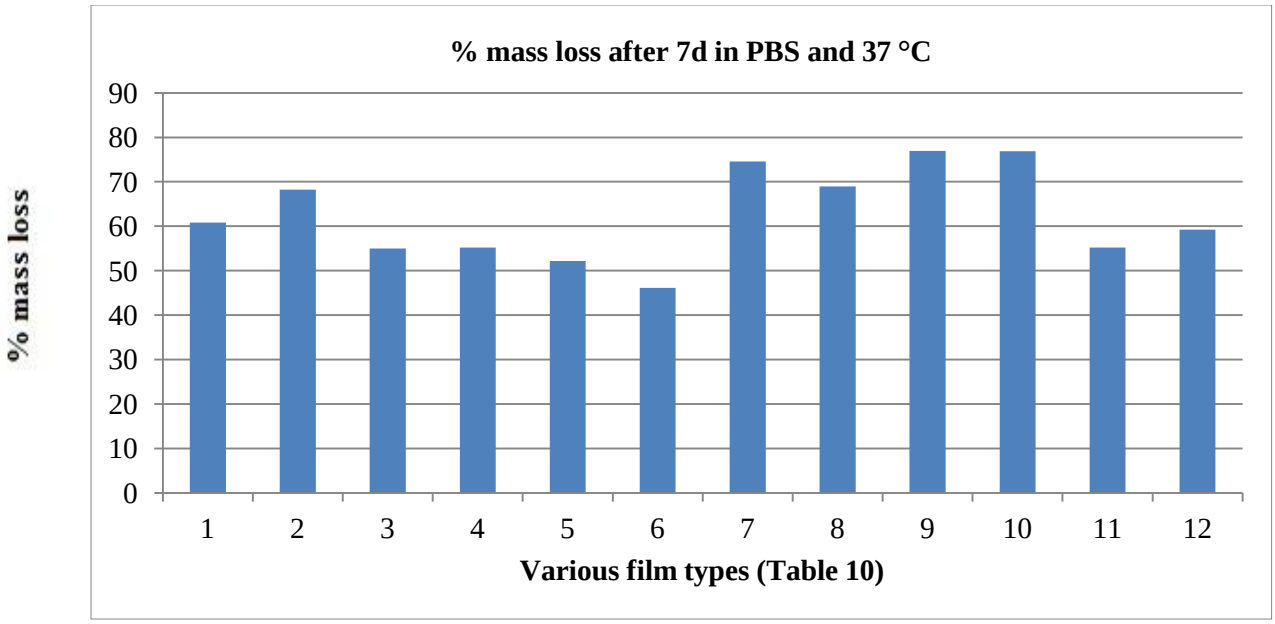

Figure 55. Percentage mass loss after 7 days in PBS at 37 °C after been immersed for 1 hr in methanol. One sample per condition was tested in all cases.

4. 16 Effect of rapid crosslinking on dissolution of films

Previous studies demonstrated that mass loss in silk film at a percentage of 50-60 % after of 7 days of incubation at 37° C (Figure 55) occurred when films are treated with methanol. The rapid crosslinking was imposed by placing the scaffolds in 60 °C for 2-3 hours [62]. Crosslinking treatment was applied to the 7 different films (Table 8). Four out of the seven films (Film 5, 6, 7 and 1) from Table 8 did not dissolve after rapid crosslinking making it feasible to measure their mass loss. Films 2, 3 and 4 were not affected by crosslinking and dissolved after rapid crosslinking. The mass loss calculations that were measured by weight in a sample of n=6 for each film showed a mass loss of 27.29 % as minimum (Figure 56).

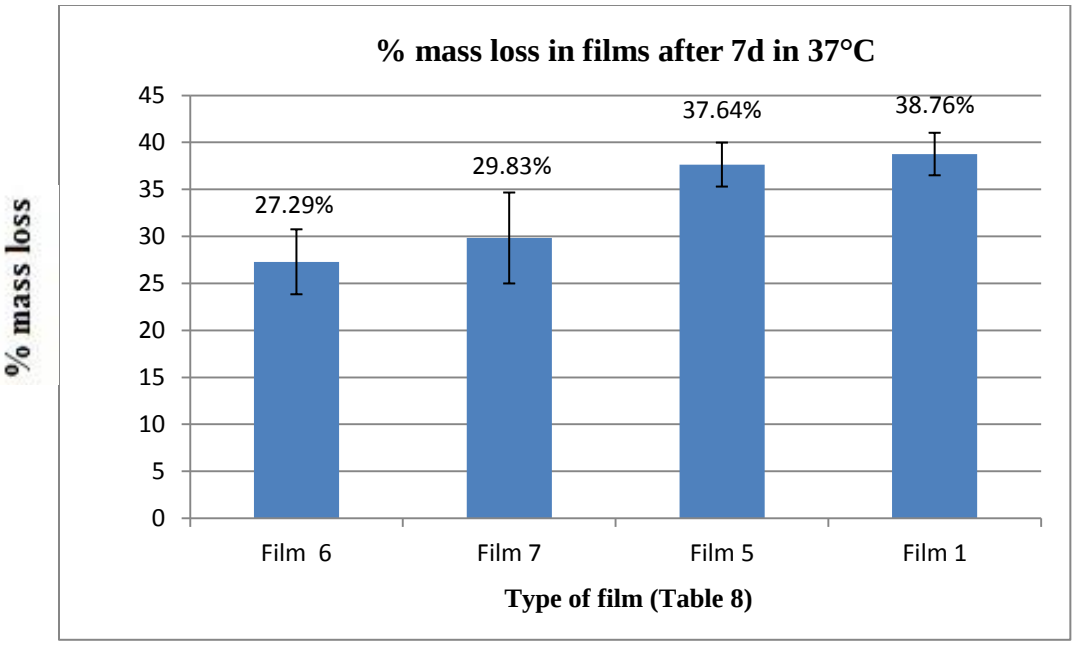

Figure 56. Percentage of mass loss in films rapidly crosslinked at 60 °C after 7d in PBS and 37 °C.

Macroscopically the films are presented in Figure 57 and Figure 58. In Figure 57 it is depicted that some of the films after 7 days in PBS and 37 °C were dissolved and decomposed (top plate). However, although the films became thinner, they maintained their shape and structure, and also limited loss of riboflavin was observed (bottom plate). We speculate that the high mass loss is due to the glycerol wash out. Yet, the results of quantifying the mass loss are contradictory to the visual observations of the films. Therefore, further analysis of the composition of the PBS solution after the seventh day is suggested.

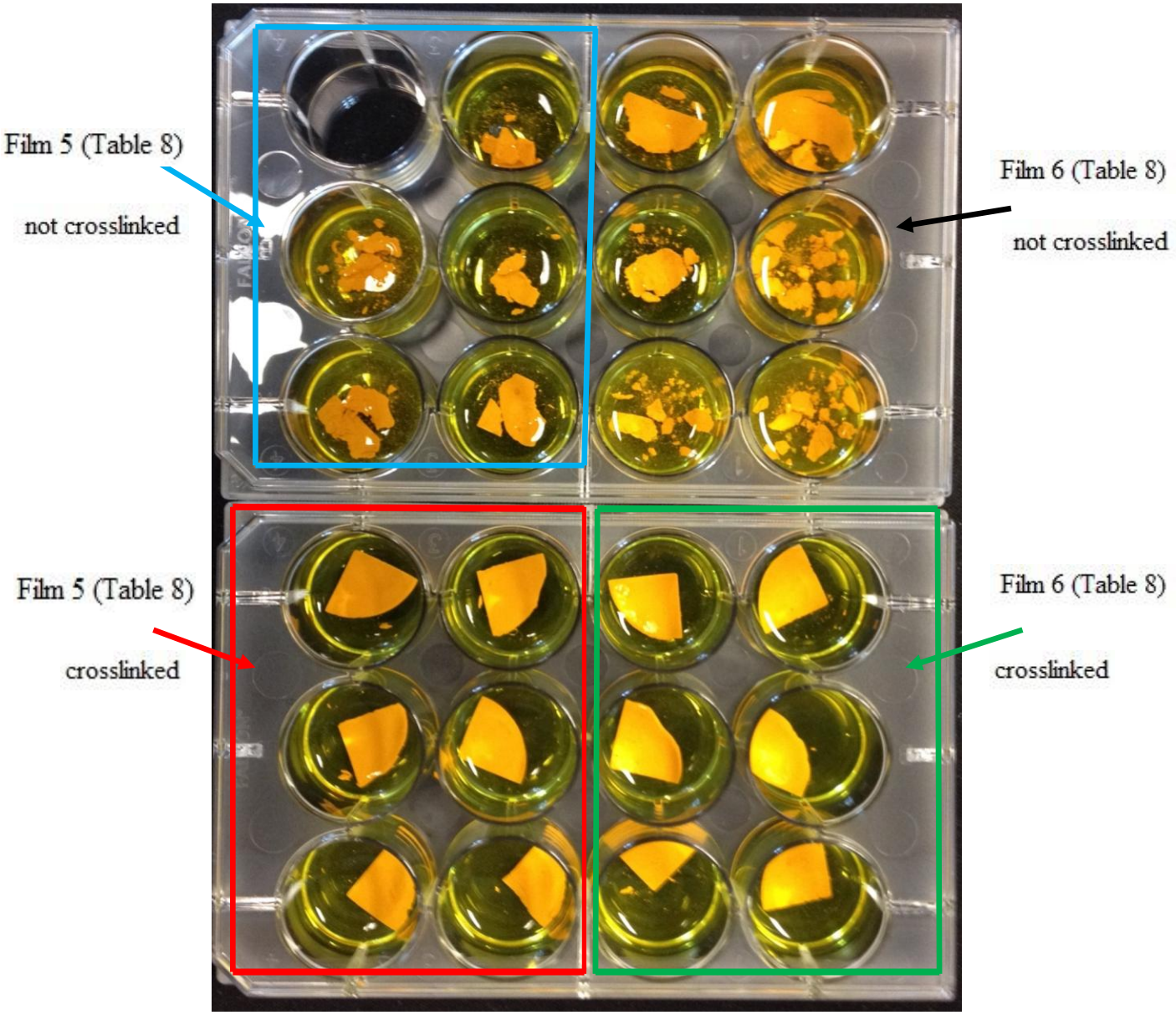

Figure 57. Comparison of mass loss in rapid crosslinked films after 7 days in PBS in 37 °C. On the top plate left are depicted the riboflavin-silk films (Film 5 from Table 8) that were not placed in 60° C for 2 hours, while on the bottom plate on the left side ar are depicted the same films that were rapidly crosslinked by being placed for 2 hours in 60° C right after casting. Respectively, on the right side are depicted riboflavin-silk films (Film 6 from Table 8) on the top that were not placed in 60° C for 2 hours, while on the bottom plate on the right side are depicted the same films that were rapidly crosslinked by being placed for 2 hours in 60° C right after casting.

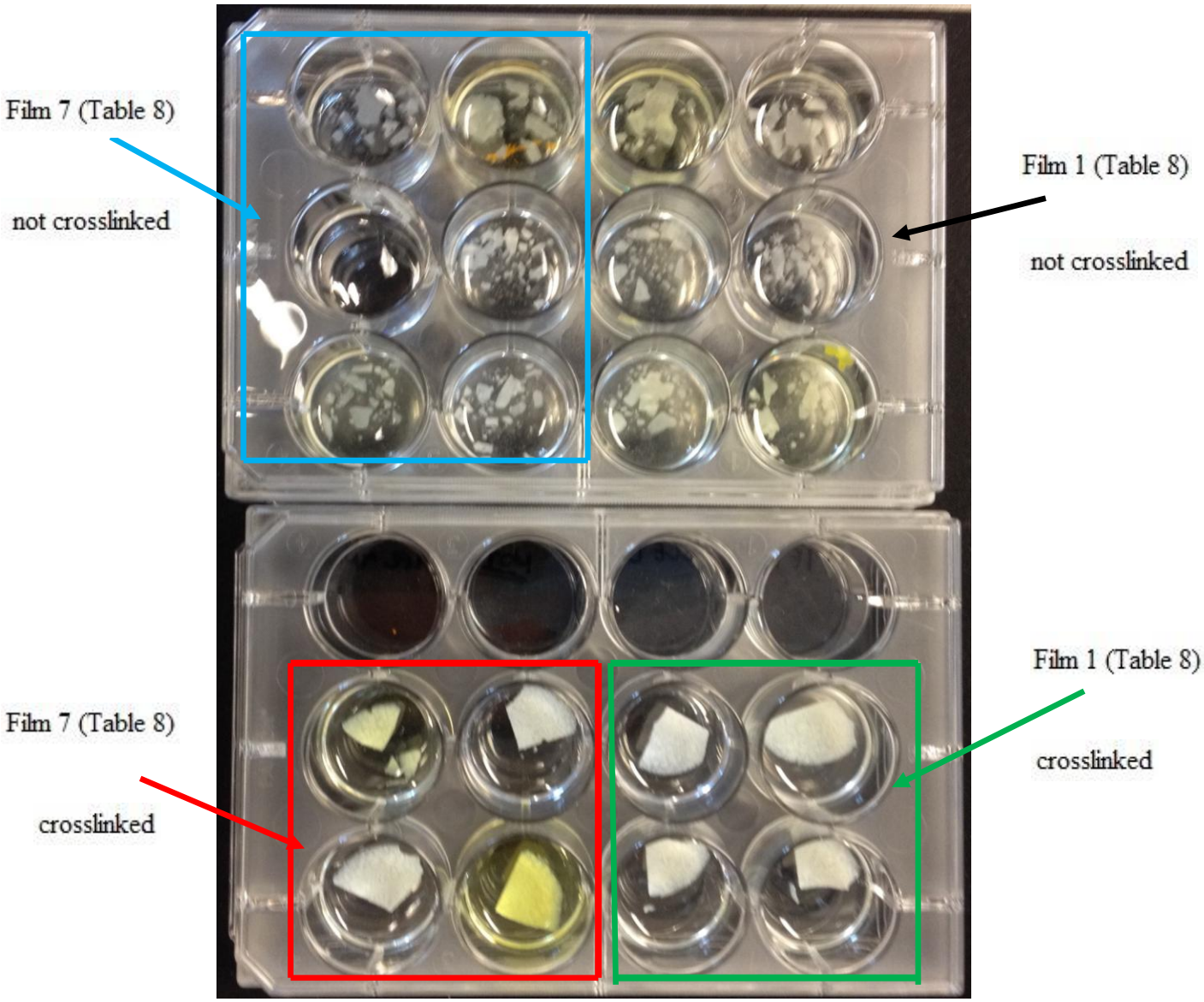

Figure 58. Comparison of mass loss in rapid crosslinked films after 7 days in PBS in 37 °C. On the top plate left are depicted the NaCl-silk films (Film 7 from Table 8) that were not placed in 60° C for 2 hours, while on the bottom plate on the left side are depicted the same films that were rapidly crosslinked by being placed for 2 hours in 60° C right after casting. Respectively, on the right side are depicted NaCl-silk films (Film 1 from Table 8) on the top that were not placed in 60° C for 2 hours, while on the bottom plate on the right side are depicted the same films that were rapidly crosslinked by being placed for 2 hours in 60° C right after casting.

Conformation and alignment of peptide chains have impact on the performance and physical properties of silk fibers and silk-fibroin based materials; therefore, it is important to be able evaluate the secondary protein structure. Water vapor annealing induces β-sheet formation in silk. Water annealing causes changes to silk molecular structure and thus, its physical properties may be altered, such as the conductivity. More specifically, after water annealing the films have the property to be insoluble but flexible. Mo et al. [85] found that the formation of β-sheets in wet films is strongly related to the dissociation of hydrogen bonds between water and peptide residues. Dissociation between water and peptides makes this transition possible [85]. In other words, water annealing is a method for controlling the crystallization of films.

5. Conclusions

Generally, electrical conductivity is a desirable property in implantable nerve conduits, and may improve nerve regeneration. Over the past decades, silk fibroin biomaterials have attracted attention due to their advantageous properties such as controllable biodegradability, biocompatibility, haemostatic properties and non inflammatory features. Normally, silk films are insulators, and do not possess conductivity. Semiconductor silk films can be fabricated with the incorporation of conducting doping compounds, followed by specific treatments to induce β-sheets formations and water insoluble films. This control of mass loss and dissolution of the films in *in vivo*-like environments plays an instrumental role in film function and integrity.

In the present study, several naturally derived doping compounds have been investigated along with various treatments and processes for the fabrication of electroconductive silk films. Semiconductor silk films were fabricated with the use of riboflavin, glycerol and NaCl blends, and with the application of water annealing treatment after casting. We analyzed the films for their conductivity as well as dissolution. The most successful film fabrication exhibited conductivity in the order of approximately $6*10^{-2}$ S/m, for a film composed of 2 % w/v silk, 20 % w/v glycerol, 2 % w/v PEO, 30 % v/v PBS. Dissolution and integrity of the films was partially controlled with the application of rapid crosslinking by raising the temperature after casting (2 hrs at 60° C). The results of the study indicated that silk films doped with naturally derived compounds have statistically significant increases in conductivity. With further improvements of the dissolution properties, these blended silk materials may be promising for future implementation in neuro tissue engineering applications.

6. Future Directions

The ultimate goal of this project is to enhance the growth of neuron and glial cells by developing electroconductive silk films that can be used as nerve guidance conduits. The film-nerve conduit will mimic the extracellular matrix in combination with biocompatible and biodegradable conjugated natural compounds, and will offer the ability to impose electrical stimuli to the cells which has been shown to increase nerve repair and regeneration.

In the future, for the case of melanin, alternative sources of melanin may be investigated, such as plant derived as well as melanin-based compounds that have improved solubility.

Another study that can be investigated more thoroughly is the silk paper-like sheet. In particular, different compositions of melanin suspension, the use of other compounds such as riboflavin with the same method can be explored.

Another study that could be conducted is the covalent modification of silk with riboflavin. The idea in this project is to take advantage possible coupling reactions of riboflavin with silk, which may maintain its electroconductive property in the conjugated material. Methods of chemically modifying silk has been extensively investigated in Professor Kaplan's lab [89]. There two candidate ways to conduct this hypothesis.

One option is the covalent binding of riboflavin to proteins via photocoupling. This methods has been accomplished for attaching riboflavin to bovine serum albumin and human serum albumin in which the maximum binding occurred at pH $\geq$ 8 [90]. Possibly, the site of attachment of the riboflavin isoalloxazine moiety (8a position) to the albumins is the Histidine residue.

The second option is the covalent coupling of the primary hydroxyl group of riboflavin with the amino groups of silk via carbonyldiimidazole. This coupling procedure has been applied to activate a hydroxyl functional group. This reaction creates an intermediate that has an -OH group and it is an imidazolyl carbamate. The attack by an amine releases the imidazole but not the carbonyl. In this way one carbon spacer and the formation of urethane linkages (N-alkyl carbamate) may be produced by the coupling [91]. To the same notion N, N-Disuccinimidyl carbonate or N-Hydroxysuccinimidyl chloroformate activation can be tried. The N, N-Disuccinimidyl carbonate will form two molecules of N-Hydroxy succinimide and also release carbondioxide in aqueous solutions. These molecules activate compounds which can be used to be conjugated with amine-containing molecules that result in stabilization of the crosslinked products [91]. Poly(lysine) silk ionomers have been recently prepared and offer a silk-based material with high amine content [92].

Additionally, AFM will be used to evaluate the stiffness of the biomaterials. Scanning electron microscopy will be also used to investigate the structure and the composition of the biomaterials. Stress/ strain assessment of the films and the determination of the Young's modulus will provide necessary data for characterizing the mechanical properties of the films. Mass spectrometry can be used to identify the leaching of glycerol and PEO in degradation studies. UV absorption can be employed to quantify the concentration of riboflavin in PBS.

Following materials characterization, cells cultures will be applied on the biomaterials to study the cells viability using metabolic assays, and also with confocal microscopy to visualize neuron adhesion and the growth of the axons. Apart from the films, the studies can be extended also using the riboflavin-silk salt-leeched scaffolds, which also exhibited conductive properties and low dissolution rates. These studies will employ electrical stimulation of various cell types (hMSC's, Schwann cell) both in 2D and 3D electroconductive films to assess the effect of stimulation on cell. Stem cell differentiation may also be studied.

Finally, the role of electrical stimulation may be investigated on drug action (tumors, neurodegenerative diseases), wound healing films, and the utilization of films as electroconductive *in vivo* patches that will monitor and record data in tissues.

7. References

1. D. Seliktar, *Designing cell-compatible hydrogels for biomedical applications.* Science, 2012, 336: p. 1124.
2. Rockwood DN, Preda RC, Yücel T, Wang X, Lovett ML, Kaplan DL. *Materials fabrication from Bombyx mori silk fibroin.* Nat. Protocols, 2011. **6**(10): p. 1612–1631.
3. C. Vepari, D. L. Kaplan, *Silk as a Biomaterial*. Progress in polymer, 2007, **32**(8-9): p. 991-1007.
4. C. A. Sundback, J. Y. Shyu, Y. Wang, W. C. Faquin, R. S. Langer, J. P. Vacanti, T. A. Hadlock, *Biocompatibility analysis of poly(glycerol sebacate) as a nerve guide material* Biomaterials 2005, **26**(27): p. 5454-64.
5. L. Meinel, S. Hofmann, V. Karageorgiou, C. Kirker-Head, J. McCool, G. Gronowicz, L. Zichner, R. Langer, G. Vunjak-Novakovic, D. L. Kaplan, *The inflammatory responses to silk films in vitro and in vivo.* Biomaterials, 2005, **26**(2): p.147-55.
6. Horan RL, Antle K, Collette AL, Wang Y, Huang J, Moreau JE, Volloch V, Kaplan DL, Altman GH. *In vitro degradation of silk fibroin.* Biomaterials, 2005, **26**(17): p.3385–3393.
7. Meinel L, Karageorgiou V, Fajardo R, Snyder B, Shinde-Patil V, Zichner L, Kaplan D, Langer R, Vunjak-Novakovic G. *Bone tissue engineering using human mesenchymal stem cells: effects of scaffold material and medium flow*, Ann Biomed Eng., 2004, 32(1): p.112– 122.
8. Meinel L, Fajardo R, Hofmann S, Langer R, Chen J, Snyder B, Vunjak-Novakovic G, Kaplan D. , Silk implants for the healing of critical size *bone* defects. *Bone*, 2005, (37) 5: p. 688-698.

9. X. Hu, X. Wang, J. Rnjak, A. S. Weiss, D. L. Kaplan, *Biomaterials derived from silk-tropoelastin protein systems.* Biomaterials, 2010, **31**(32): p.8121-31

10. B. An, T. M. DesRoechers, G. Qin, X. Xia, G. Thiagarajan, B. Brodsky, D. L. Kaplan, *The influence of specific binding of collagen-silk chimeras to silk biomaterials on hMSC behavior*. Biomaterials 2013, **34**(2): p. 402-12.

11. X. Hu, K. Shmelev, L. Sun, E. S. Gil, S. H. Park, P. Cebe, D. L. Kaplan, *Regulation of silk material structure by temperature-controlled water vapor annealing.* Biomacromolecules, 2011, **12**(5): p. 1686-96.

12. Karageorgiou V, Meinel L, Hofmann S, Malhotra A, Volloch V, Kaplan D. *Bone morphogenetic protein-2 decorated silk fibroin films induce osteogenic differentiation of human bone marrow stromal cells.* J Biomed Mater Res A, 2004, **71**(3): p. 528-537

13. Sofia S, McCarthy MB, Gronowicz G, Kaplan DL. *Functionalized silk-based biomaterials for bone formation.* J Biomed Mater Res 2001, 54(1): p. 139-148.

14. Jin HJ, Park J, Valluzzi R, Cebe P, Kaplan DL. *Biomaterial films of Bombyx mori silk fibroin with poly(ethylene oxide).* Biomacromolecules, 2004, **5**(3): p.711-717.

15. Labes MM, Love P, Nichols LF. *Polysulfur nitride-a metaillic, superconducting polymer*. Chem Rev, 1979, **79**(1): p.1-15

16. Richard Balint, Nigel J. Cassidy, Sarah H. Cartmell, *Conductive polymers: Towards a smart biomaterial for tissue engineering.* Acta Biomater. 2014, **10**(6): p. 2341-53.

17. Nectow AR[1], Marra KG, Kaplan DL. *Biomaterials for the development of peripheral nerve guidance conduits* , Tissue Eng Part B Rev. 2012, **18**(1): p. 40-50.

18. Heeger A.J, Macdiarmid G.A. and Shirakawa H. , Conductive Polymers, the nobel Prize in Chemistry 2000, Kungl. Vetenskapsanakademin, p.1-16.

19. R. E. Hummel, *"Electronic Properties of Materials",* 3rd ed., Springer, New York, 2001, 18-20, p. 77-87.

20. A. Moliton, *Ion implantation doping of electroactive polymers and device fabrication in "Handbook of Conducting Polymers*", 2nd ed., ed. T.A. Skotheim, R.l. Elsenbaumer, J.R. Reynolds, Marcel Dekker, Inc., New York, 1998: p. 589- 638.

21. G. Zotti, *Electrochemical synthesis of polyheterocycles and their applications, in* "*Handbook of Conductive Molecules and Polymers",* Vol. 2, ed. H.S. Nalwa, J.Willey

22. A. R Blythe, "*Electrical Properties of Polymers"*, Cambridge University Press, Cambridge, 1979: p. 132-138.

23. Inzelt, G., *"Conducting Polymers. Monographs in Electrochemistry",* ed. F. Scholz. 2008, Berlin Heidelberg: Springer.

24. H. R. Allcock, F. W. Lampe, J. E. Mark, *"Contemporary polymer chemistry",* (3rd ed.), Pearson Education, Inc, USA, 2003: p. 717-728.

25. MacDiarmid, A.G., Synthetic metals: A novel role for organic polymers. Synthetic Metals, 2002, **125**(1): p. 11-22.

26. Prasanna Chandrasekhar, *"Conducting Polymers, Fundamentals and Applications: A Practical Approach"*, Massachusetts: Kluwer Academic Publishers, 1999.

27. Ashwell, G. J., Ed. *"Molecular Electronics"* Research Studies Press: Somerset, 1992

28. Aldissi M. *"Inherently Conducting polymers"*, Noyes Data Corporation: New Jersey, 1989.

29. Salaneck, W. R. ; Lundstrom, I.; Ranby, B., Eds. *"Conjugated polymers and related materials: the interconnection of chemical and electronic structure"*, Oxford University Press: New York 1993.

30 . Naarman, H. *"Science and applications on condunting polymers"* Adam Hilger, Publ.: Bristol, 1991.

31. A B Kaiser *"Electronic transport properties of conducting polymers and carbon nanotubes"* 2001 *Rep. Prog. Phys.* **(64)**1.

32. Ghaznavi AM[1], Kokai LE, Lovett ML, Kaplan DL, Marra KG.Silk fibroin conduits: a cellular and functional assessment of peripheral nerve repair, Ann Plast Surg. 2011, **66**(3):273-9.

33. Yang Y1, Chen X, Ding F, Zhang P, Liu J, Gu X, *Biocompatibility evaluation of silk fibroin with peripheral nerve tissues and cells in vitro,* Ann Plast Surg. 2007, **28**(9): p. 1643-52.

34. Georgiou M1, Bunting SC, Davies HA, Loughlin AJ, Golding JP, Phillips JB. *Engineered neural tissue for peripheral nerve repair*. Biomaterials, 2013, **34**(30): p.7335-43.

35. http://bme240.eng.uci.edu/students/06s/jdiomamp/biomaterial.htm

36. Hang Y, Zhang Y, Jin Y, Shao H, Hu X , *Preparation of regenerated silk fibroin/silk sericin fibers by coaxial electrospinning*. Int J Biol Macromol. 2012, **51**(5): p.980-6.

37. M. Muskovitch & Bettinger CJ. *Biomaterials-Based Electronics: Polymers and Interfaces for Biology and Medicine.* Adv Healthc Mater. 2012, **1**(3): p. 248–266.

38. Bettinger CJ et al. *Biocompatibility of biodegradable semiconducting melanin films for nerve tissue engineering*. Biomaterials, 2009, **30**(17): p. 3050-7.

39. M. Abbas et al. *Structural, electrical, electronic and optical properties of melanin films.* The European Physical Journal, 2009, **28**(3) : p. 285-291.

40. MR Abidian. *Hybrid Conducting Polymer–Hydrogel Conduits for Axonal Growth and Neural Tissue Engineering*. Adv Healthc Mater, 2012, **1**(6) : p. 762-7

41. K Svennersten. *Organic bioelectronics in nanomedicine*. Biochim Biophys Acta, 2011, **1810**(3) : p. 276-85.

42. George G. Malliaras. *Organic bioelectronics: A new era for organic electronics*. Biochimica et Biophysica Acta (BBA), 2013, **1830**(9): p. 4286-4287.

43. Sharon L. Bourke & Joachim Kohn, *Polymers derived from the amino acid L-tyrosine: polycarbonates, polyarylates and copolymers with poly(ethylene glycol).* Advanced Drug Delivery Reviews, 2003, 55: p. 447-466.

44. C. Meechaisue et al. *Electrospun mat of tyrosine-derived polycarbonate fibers for potential use as tissue scaffolding material*. J. Biomater. Sci. Polymer, 2006, **17**(9) : p. 1039–1056.

45. M. Puma et al. *Conductivity and High-Temperature Relaxation of Tyrosine-Derived Polyarylates Measured with Thermal Stimulated Currents*, Journal of Polymer Science Part B: Polymer Physics, 1999, **37**(24) : p. 3504–3511.

46. P Humpolicek et al. *Biocompatibility of polyaniline.* Synthetic Metals, 2012, **162** (7-8) : p. 722-727.

47. Mahmoud Roushani', Zeinab Abdi. *Novel electrochemical sensor based on graphene quantum dots/riboflavin nanocomposite for the detection of persulfate*. Sensors and Actuators B: Chemical, 2014, 1 : p. 503-510.

48. S. Ashok Kumar, Shen-Ming Chen. *Electrochemically polymerized composites of conducting poly(p-ABSA) and flavins (FAD, FMN, RF) films and their use as electrochemical sensors: A new potent electroanalysis of NADH and NAD+*. Sensors and Actuators B, 2007, 123: p. 964–977.

49. J. McGinness, P. Corry, P. Proctor, *Amorphous semiconductor switching in melanins.* Science, 1974, 183 : p. 853-855.

50. Strzelecka T. *Semiconductor properties of natural melanins*. Physiol Chem Phys. 1982, **14**(3): p. 223-31.

51. Strzelecka T. *A hypothetical structure of melanin and its relation to biology*. Physiol Chem Phys. 1982, **14**(3): p. 233-7.

52. Strzelecka T. *A band model for synthetic dopa-melanin,* Physiol Chem Phys. 1982, **14**(3): p. 219-22.

53. Osak, W., K. Tkacz, H. Czternastek and J. Slawinski. *I-V characteristics and electrical conductivity of synthetic melanin*. Biopolymers, 28, : p.1885-1890.

54. Jastrzebska, M., A. Kocot and L. Tajber (2002) *Photoconductivity of synthetic dopa-melanin polymer*. J. Photochem. Photobiol. B, Biol. 2002, 66: p. 201-206.

55. Lundstrom I. Svensson S. *Natural nanosystems*. Current Applied Physics 2002, 2: p. 17-21.

56. Rosei, M. A., L. Mosca and F. Galluzzi, *Photoelectronic properties of synthetic melanins*. Synth. Met., 1996, 76 : p. 331-335.

57. Mason H.S Advances in Biology of Skin. 1967, 8: p. 293-312.

58. Jartzebska, M Isotalo H. Paloheimo, J Stubb, H. *Electrical conductivity of synthetic DOPA-melanin polymer for different hydration states and temperatures*. Journal of Biomaterials Science. Polymer Edition, 1995, 7: p.577-586.

59. Pezzella, A Napolitano A, d' Ischia, M Prota, G. *New pyrrole acids by oxidative degradation of eumelanins with hydrogen peroxide. Further hints to the mechanism of pigment breakdown*. Tetraehedron, 1996, 52: p. 7913-7910.

60. Wang ZX, Zhuge J, Fang H, Prior BA. Glycerol production by microbial fermentation: a review. Biotechnol Adv. 2001, **19**(3) : **p.** 201-23.

61. Tsukada S, Nakashima H, Torimitsu K., Conductive polymer combined silk fiber bundle for bioelectrical signal recording. PLoS One. 2012, **7**(4).

62. Lu et al. *Insoluble and Flexible Silk Films Containing Glycerol*. Biomacromolecules. 2010, **11**(1): p. 143-50.

63. Haesung Yun *et al*. *Preparation and characterization of silk sericin/glycerol/graphene oxide nanocomposite film.* Fibers and Polymers, 2013, **14**(12) : p. 2111-2116.

64. Hurrell R, Egli I. *Iron bioavailability and dietary reference values*. Am J Clin Nutr 2010, 91: p. 1461S-7S.

65. Institute of Medicine. Food and Nutrition Board. Dietary Reference Intakes for Vitamin A, Vitamin K, Arsenic, Boron, Chromium, Copper, Iodine, Iron, Manganese, Molybdenum, Nickel, Silicon, Vanadium, and Zinc : a Report of the Panel on Micronutrients. Washington, DC: National Academy Press; 2001.

66. Lu Q, Zhang B, Li M, Zuo B, Kaplan DL, Huang Y, Zhu H. *Degradation mechanism and control of silk fibroin,*. Biomacromolecules. 2010, 12(4): p. 1080-6.

67. Laurent S, Forge D, Port M, Roch A, Robic C, Vander Elst L, Muller RN., *Magnetic iron oxide nanoparticles: synthesis, stabilization, vectorization, physicochemical characterizations, and biological applications*. Chem Rev. 2008 **108**(6): p. 2064-110.

68. Soner Çakmak, Menemse Gümüsderelioglou, Adil Denizli, *Biofunctionalization of magnetic poly(glycidyl methacrylate) microspheres with protein A: Characterization and cellular interactions*. Reactive & Functional Polymers 2009, 69: p. 586–593.

69. Ciobanu CS et al**.** *Biomedical properties and preparation of iron oxide-dextran nanostructures by MAPLE technique*. *Chemistry Central Journal*, 2012, **6**:17.

70. Partlow BP. *et al.* Highly tunable elastomeric silk biomaterials, Advanced Functional Materials, 2014, **24**(29): p. 4615–4624.

71. Liang B, Fang L, Hu Y, Yang G, Zhu Q, Ye X. *Fabrication and application of flexible graphene silk composite film electrodes decorated with spiky Pt nanospheres*. Nanoscale. 2014, **6**(8): p. 4264-74.

72. Hronik-Tupaj M, Raja WK, Tang-Schomer M, Omenetto FG, Kaplan DL. *Neural responses to electrical stimulation on patterned silk films*. J Biomed Mater Res A. 2013 **101**(9): p. 2559-72.

73. http://edn.com/design/test-and-measurement/4411117/Two-wire-vs--four-wire-resistance-measurements.

74. Kirk T. McDonald, *Resistance of a Disk,* 2000, Joseph Henry Laboratories, Princeton University, Princeton.

75. Handbook of Thin Film Process Technology, Editors: D. A. Glocker and S.I. Shah, Institute of Physics Publishing, Bristol and Philadelphia, 1998.

76. Norrman, K., A. Ghanbari-Siahkali, and N.B. Larsen, *Studies of spin-coated polymer films*. Annual Reports on the Progress of Chemistry - Section C, 2005, 101: p. 174-201.

77. L. Huang, K. Nagapudi, R. P. Apkarian, E. L. Chaikof, J. *Engineered collagen-PEO nanofibers and fabrics*. Biomater. Sci. Polym. Ed. 2001, 12: p. 979 – 993.

78. Greiner A, Wendorff J.H, *Electrospinning: A Fascinating Method for the Preparation of Ultrathin Fibers*, Angew. Chem. Int. Ed. 2007, 46: p. 5670-5703.

79. G. Toskas, R.-D. Hund, E. Laourine, and Ch. Cherif, *Nanofibers from Natural Biopolymers in Regenerative Medicine*, 2012, chapter 5, in Book "Textiles: Types, Uses and Production Methods" by Nova Science Publishers, New York, USA.

80. G. Howatt, R. Breckenridge, *Fabrication of Thin Ceramic Sheets for Capacitors, J. Brownlow*, 1947, J. Am. Ceram. Soc., 30, 237.

81. G. N. Howatt, Method of Producing High-Dielectric High-Insulation Ceramic Plates, US Patent 2582993.

82 . Wang X, Kluge JA, Leisk GG, Kaplan DL. *Sonication-induced gelation of silk fibroin for cell encapsulation*. Biomaterials. 2008, **29**(8): p.1054-64.

83. Sangram K.S, Kaplan DL, Chiellin E, *Ultrasound Sonication Effects on Silk Fibroin Protein*. 2013, **298**(11), : p. 1201–1208.

84. Lawrence BD, Wharram S, Kluge JA, Leisk GG, Omenetto FG, Rosenblatt MI, Kaplan DL., *Effect of hydration on silk film material properties*. Macromol Biosci. 2010, **10**(4): p. 393-403.

85. C. Mo, P. Wu, X. Chen, and Z. Shao, *The effect of water on the conformation transition of Bombyx mori silk fibroin.* Vibrational Spectroscopy, 2009, **51**(1), : p. 105-109.

86. Inoue, S.I , Magoshi, J., Tanaka , T., Magoshi Y, Becker M. *Atomic force microscopy: Bombyx mori silk fibroin molecules and their higher order structure*. Journal of Polymer Science Part -B Physics, 2000, 38 : p. 1436-1439.

87. Moore AM, Kasukurthi R, Magill CK, Farhadi HF, Borschel GH, Mackinnon SE *Limitations of conduits in peripheral nerve repairs.* Hand (NY), 2009, **4**(2): p. 180-6.

88. http://ods.od.nih.gov/factsheets/Iron-HealthProfessional/

89. Amanda R. Murphy and David L. Kaplan, *Biomedical applications of chemically-modified silk fibroin,* J Mater Chem. 2009, **19**(36):6443-6450.

90. Carmichael, Richard Gay, *Photoinduced covalent coupling of riboflavin to bovine and human serum albumins: preparation of model compounds for covalently linked flavoproteins.* Master of Science Thesis, 1976, Texas Tech University.

91. Greg Hermanson, Bioconjugate Techniques, Academic Press, 2008, 2nd ed.

92. Rossella Calabrese and David L. Kaplan, *Silk ionomers for encapsulation and differentiation of human MSCs*, Biomaterials, **33**(30): 7375–7385.